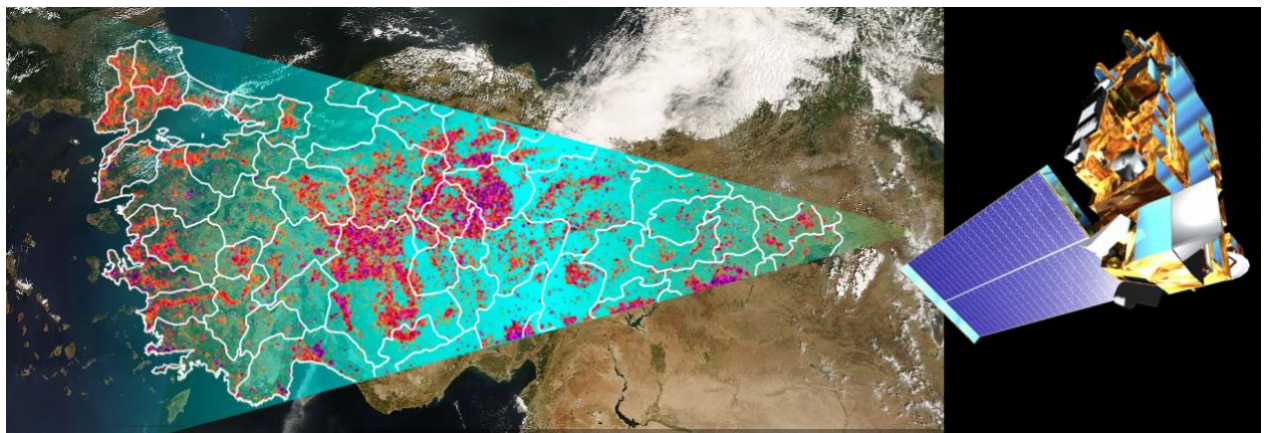




Co-funded by the  
Erasmus+ Programme  
of the European Union



## Describing fire regimes over Turkey using MODIS fire observations



### Supervisors

Prof. Jose M.C. Pereira, ISA

Prof. Pedro Silva, ISA

Prof. Jose Antonio Bonet, UdL

**Giuseppe Baldassarre**

04/01/2021



**The University of Lleida**  
**School of Agrifood, Forestry Science and Engineering**

**Describing fire regimes over Turkey using MODIS fire  
observations**

**Supervised by**

Prof. Jose M.C. Pereira, ISA

Prof. Pedro Silva, ISA

Prof. Jose Antonio Bonet, UdL

**Submitted by**

Giuseppe Baldassarre

# Table of Contents

<b>Abstract.....</b>	<b>7</b>
<b>1 Introduction.....</b>	<b>9</b>
<b>2 Materials and Methods.....</b>	<b>11</b>
2.1 Study Area .....	11
2.2 Fire issues in Turkey .....	19
2.3 Satellite Data.....	20
2.4 Fire Regime variables .....	22
2.5 Description of the spatial patterns of the MODIS data.....	30
2.6 Principal Component Analysis (PCA).....	32
2.7 Hierarchical Agglomerative Cluster (HAC) analysis .....	33
<b>3 Results .....</b>	<b>34</b>
3.1 Principal Component Analysis (PCA).....	34
3.2. Clusters and classification of fire regimes .....	39
3.3. Sensu lato fire regime characterization: anthromes and climate types .....	44
<b>4 Discussion.....</b>	<b>48</b>
4.1 Fire regime characteristics and their main drivers .....	48
<b>5 Conclusions.....</b>	<b>51</b>
<b>References .....</b>	<b>53</b>
<b>Appendices.....</b>	<b>59</b>
<b>Appendix A: Turkish Province IDs and MODIS active fire counts.....</b>	<b>59</b>
<b>Appendix B: Season Length (SL) and Season Modality (SM) calculation .....</b>	<b>60</b>
<b>Appendix C: Sensu Stricto and Sensu Lato variables .....</b>	<b>62</b>
<b>Appendix D: Correlation between the quantitative variables .....</b>	<b>63</b>

## Figure Index

Fig. 1. The four phytogeographical regions of Turkey: Euro-Siberian, Mediterranean, Iran-Turan and Mesopotamian (after (I. Atalay, 1986)). .....	12
Fig. 2. Land use/cover classes (Label1) visualized with 100 m resolution (CLC 2018). In the table on the left, first 20 largest Turkish cities with their relative population (Turkish Statistic Institute, 2020). .....	15
Fig. 3. (a) Forest types (Label3). (b) Steppes and Scrub types (Label3). (c) Agricultural area types (Label2). (d) Arable Land types (Label3). Visualized with 100 m resolution (CLC 2018). .....	16
Fig. 4. Anthropogenic biomes in Turkey according to the Anthromes Working Group classification. (a) Aggregated classes (1990). (b) Aggregated classes (2015). (c) Croplands (1990). (d) Croplands (2015). Visualized with 500 m resolution (Özşahin & Eroğlu, 2020). .....	16
Fig. 5. (a) The 7 geographical regions of Turkey and the 81 provinces on Land use/cover classes visualized with 100 m resolution. (b) Percentage of the land cover/use classes in each geographical region. (CLC 2018) .....	18
Fig. 6. The EFFIS fuel map. Fuel categories of the Northern Forest Fire Laboratory (NFFL) or fire behavior models (Anderson, 1982). .....	20
<i>Fig. 7. MODIS active fires (2003-2019) ordered by FRP (a). MODIS burned area (2003-2019) ordered by the month of the year it was detected (b). Below the percentage referring to the classes identified by respective colors. ....</i>	<i>22</i>
Fig. 8. Maps of fire incidence (a, b) and its inter-annual variability (c, d) in Turkey based on MODIS active fire data (a, c) and burned area data (b, d). .....	24
Fig. 9. Maps of fire season duration (a), fire season modality (b), and percentage of yearly fire peak month that belong to the summer period (June to September) (c), fire peak month (d), and fire intensity (e) in Turkey based on MODIS active fire data. ....	25
<i>Fig. 10. Anthropogenic biomes in Turkey according to the Anthromes Working Group classification. (a) Anthromes 12K map of 2015 - Aggregated classes. (b) Adapted map of 2015 - Aggregated classes (2015). (c) Anthromes 12K map of 2015 - Croplands. (d) Adapted map of 2015</i>	

- Croplands). Anthromes 12K maps are visualized with 5' (ca. 8km) resolution while the Adapted maps are visualized with 500 m resolution. ....	28
Fig. 11. Map of the dominant Anthromes (Aggregated classes) for each provinces (%), based on the adapted map for 2015 (Özşahin & Eroğlu, 2020). When the difference between the 1 <sup>st</sup> and 2 <sup>nd</sup> most extensive Anthrome is less then 10% both classes are reported with their relative percentage (%) under the category “Other” in white. (Vi: Villages; Wi: Wildlands; Cr: Croplands; Ra: Rangelands; Fo: Forests). ....	28
Fig. 12. Map of the dominant Cropland types for each provinces (%), based on the adapted map for 2015 (Özşahin & Eroğlu, 2020). When the difference between the 1 <sup>st</sup> and 2 <sup>nd</sup> most extensive type is less then 10% both classes are reported with their relative percent (%) under the category “Other” in white. (RI: Residential Irrigated; RR: Residential Rainfed; PR: Populated Rainfed; Rm: Remote). ....	29
Fig. 13. Köppen climate types of Turkey. Adapted map visualized with 1 km resolution (Yılmaz & Çiçek, n.d.). (B: Arid; Cf: Temperate, w/out dry summer; Cs: Temperate, dry summer; Df: Cold, w/out dry summer; Ds: Cold, dry summer ). ....	29
Fig. 14. Map of the dominant Climate types for each provinces (%), based on the adapted map (Yılmaz & Çiçek, n.d.). When the difference between the 1st and 2nd most extensive Climate type is less then 30% both types are reported with their relative percent (%) under the category “Other” in white. ....	30
Fig. 15. MODIS active fires (2003-2019) ordered by Anthromes – Aggregated classes (a), Anthromes – Croplands (b) and by Köppen climate types (c). ....	32
Fig. 16. Graphical representation of the percentages of variance that each PC accounts for together with the scree plot of the cumulative percentage of explained variance. ....	35
Fig. 17. Correlation spheres. ....	39
Fig. 18. Dendrogram produced by the hierarchical clustering method applied to the first four PCs. The vertical axis represents the merging costs defined by Ward's method. ....	40
Fig. 19. Scatter plots of the observations within their convex envelopes, colored according to the clusters they belong to. These observations are projected on the factorial space, defined by: (a) the first two PCs, (b) the first three PCs, (c), the first two and the fourth PC. ....	42

*Fig. 20. Value distributions of fire regime variables. The black dot indicates the median, whereas the left and right edges of the colored box indicate the 25th and 75th percentiles, respectively. The colored circles indicate outliers..... 43*

*Fig. 21 low incidence, medium-long (often multi-unimodal) seasons, medium (A1) low (A2) interannual variability of recorded burned area; B: medium incidence, medium-short (unimodal) seasons, with more intense, highly variable and predominantly summer activity ..... 44*

*Fig. 22. Percentage of total area (a), number of active fire (b) and total area burned (c) that belongs to each of the three fire regimes..... 44*

*Fig. 23. Scatter plots of the observations within their convex envelopes, colored according to the clusters they belong to, projected in the space of: (a) the first two PCs, (b) the first three PC, (c) the first two and the fourth PC. The modalities of the antecedent variables are projected in the centroids of the units having these modalities and identified by black and orange circle respectively for Anthromes - aggregated classes and Anthromes - Croplands and by magenta squares for the Köppen climate types. The size of the dots representing the modalities of the antecedent variables is proportional to the percentage of the total number of units each modality represents. .... 46*

## **Table Index**

**Tab. 1. Total surface of the main (Label1) land use/cover classes (km<sup>2</sup>) for 1990 and 2018, and the percentage of net change in land cover from 1990 to 201. (CLC 1990 and 2018)..... 15**

**Tab. 2. List of sensu strictu variables: CoV = Coefficient of Variance..... 25**

**Tab. 3. Each eigenvalue corresponds to a PC variance, and each PC to a linear combination of the initial (standardized) variables, and all the PCs are uncorrelated. The eigenvalues and the corresponding PCs are sorted by decreasing order their explained variance. The last column represents the cumulative percentage of explained variance. .... 35**

**Tab. 4. Coefficients (loadings) table ..... 36**

**Tab. 5. Correlations between variables and factors ..... 36**

**Tab. 6. Fire characteristics and classification of the fire regimes..... 47**

## **Abstract**

The MODerate resolution Imaging Spectrometer (MODIS) sensor on board of TERRA and AQUA satellites has already been employed successfully to study fire regime characteristics and their potential drivers at the global and the regional level. Here we propose a mapping of fire regimes over Turkey by taking advantages of the most recent versions of both the active fire (MCD14ML) and burned area (MCD64A1) products derived from the MODIS sensor during the period from 2003 to 2019.

Using these two datasets we computed eight fire regime variables at the spatial resolution of the Turkish provinces: incidence, inter-annual variability, seasonality and intensity. Furthermore, we characterized the Turkish provinces in terms of two antecedent variables, anthromes and climate types, using adapted high resolution maps recently released.

By mean of principal component analysis and hierarchical clustering we reduced the dimensionality of the fire regime variables and identified three main groups of provinces with distinct characteristics. Then we further characterized these groups with the antecedent variables in order to infer anthropic and climatic drivers.

Three out of four of the MODIS active fires were detected in croplands, suggesting regular use of fire as land management tool. Two out of three of the cropland active fires were recorded in residential irrigated croplands, underling the role of the percentage of rural population and water availability in boosting the agricultural burning dynamics. Three out of four the MODIS active fires were recorded in temperate dry-summer climate while irrelevant burning activity was observed over the cold and humid Black Sea provinces.

Half of the observed activity was recorded in only five of the eighty-one Turkish provinces, between Central and South-Est Anatolia, mainly coinciding with patterns of residential irrigated croplands, and characterized by regular, unimodal, summer seasons. Fires in the cold and dry croplands and rangelands of Central and East Anatolia are concentrated in short, irregular fire seasons with peak activity during the summer. The more populated provinces of West Anatolia, dominated by croplands and forests in temperate climate are characterized by more regular and longer fire season, often bi-modal with main peak in non-summer months, and low energetic occurrences. Energetic forest fires area associated with the Mediterranean forests of South Anatolia in summer time. Here climate change dynamics is increasing the risk of large episodes.

Keywords: Fire regimes, Remote sensing, MODIS, Principal component analysis, Cluster analysis, Fire drivers, Turkey, Pyrogeography

# 1 Introduction

Due to its particular geographical location, Turkey landscape is a result of a deep transformation by different civilizations on the natural biomes, since the beginning of the history. According to the most recent archeological findings, Göbekli Tepe ("Potbelly Hill" in Turkish), in the Turkish province of Sanliurfa is the first archeological proof of the beginning of the Agricultural Revolution, which resulted into the transformation of our species from hunter-gatherers into farmers, and the beginning of a long history of manipulation of natural ecosystems over the whole landmass (Harari, n.d.). The use of fire has represented one of the main tool of this process, employed to transform naturally vegetated areas into pasture and croplands, boost the cycle of nutrients and manage shrub an weed invasion (Andreae, 1993). For this reason the characterization of pyrogeographical patterns is deeply connected with the necessity to understand the interactions between dominant drivers of fire regimes (climate, vegetation and landscape) and the influence of the anthropogenic factors (Barros & Pereira, 2014).

Satellite remote sensing provides powerful means of locating and characterizing open-vegetation burnings. And it provides the only automated method capable of continuously do it at the global level (Dozier, 1981). Studies of fire regimes of large geographical areas are mainly based on remotely sensed imagery.

At the moment, the MODIS Products are the most consolidated and a reference for global Earth observation of biomass burning (Giglio, Csiszar, & Justice, 2006) and they have already been used to infer fire regimes at global (Chuvieco, Giglio, & Justice, 2008), and regional scale (Chen, Pereira, Masiero, & Pirotti, 2017).

Vegetation fires in Turkey have been studied almost exclusively on the forested areas of the Mediterranean coastline and mainly with respect to wild fires, which are those mainly reported by forest agencies at the provincial and regional level. But biomass burning is a broader phenomenon. For example, at the end of the summer, it is common practice in the agricultural to burn croplands after the harvest.

In recent years, the abandonment of agricultural lands and the encroachment upon wildlands play an important role in characterizing wildfires in Turkey (Tolunay & Türkoğlu, 1997). Furthermore, unfinished cadastral records of the wildland–urban interfaces and the centralized firefighting strategy resulted in to the use of forest fires as a mean to expands the national land market (Ertugrul & Varol, 2015). Even so, studies on land use/cover changes in the Mediterranean Turkey found no

evidence that these pressures made the landscape more hazardous as there was a net decrease in fuels biomass and the landscape became more fragmented over time.

Despite wildland areas being heavily used and relatively fragmented, large fires can occur driven by severe weather (Balaban & Fu, 2014). In fact, study of records of large fires (greater than 300 ha), more than 50% of which occur in the Aegean region of Izmir and Mugla and in the Mediterranean region of Antalya, have shown an increase in size from an average of 550 ha in the 1970s to 960 ha in 2009, with a fire cycle of 6-9 years (Varol, Ertuğrul, & ÖZEL, 2018). Trends of burned area derived via statistical quality control method using fire data from National Directorate General of Forestry from 1988 to 2015 show that: “exist a risk of burning of large areas due to the climate change conditions caused by an upward trend in the temperatures of summer months for Mediterranean Turkey and a downward trend in both total annual precipitation and summer precipitation along with the socio-economic factors” (Ertuğrul & Varol, 2016). Temperature and relative humidity are the weather variables mostly correlated with the fire activity probability (Varol et al., 2018).

Only focusing on Mediterranean Turkey, and using MODIS fire activity data from 2000 to 2015 Kavgaci et al. (2008) found that “cropland fires have a significant effect on the output of fire regime models” concluding that, in order to have a better understanding of natural fire activity “a clear distinction should be drawn between wildland and cropland fires”.

In the present study we will extend this concept by investigating which typology of biomass burning is shaping the fire regime in each of the Turkish provinces by describing their main features. Our research objectives are to characterize fire regimes over Turkey and to embed the description of the pyrogeographical patterns in a more comprehensive analysis of the complex interaction between anthropogenic and environmental drivers. With doing so we aim to provide valuable information to understand how these patterns can change in response to environmental and human drivers for better informed policies and natural resource management.

## 2 Materials and Methods

### 2.1 Study Area

#### *Phytogeographical features*

With a size of around 783,356 square kilometers, Turkey is the 36th largest country in the world (Ustaoglu & Aydinoglu, 2019). It consists of the European Turkey (the Thrace region, accounting for the 3% of the land area) and the Anatolian peninsula. The last one is basically a plateau (half of it above 1000 m and 10% above 2000 m), rising steadily towards the east and bounded to the north by the northern Anatolian mountains (a continuation of the Carpathian-Balkan mountain chains) and to the south by the Taurus mountains (eastern extensions of the Alps)(Çolak & Rotherham, 2006).

The Country is the meeting place of four phytogeographical regions, whose vegetation reflects differences in climate, geology, topography, soils and floristic diversity: the Euro-Siberian, the Mediterranean, the Iran-Turan and the Mesopotamian region (Fig. 1) (Atalay, 1986).

In contrast to most of the country, the **Euro-Siberian** region (northern part) is characterized by a very wet climate, particularly in the east, with heavy precipitation occurring all year long and annual mean ranging between 1500 and 2200 mm. In the forests of Northern Anatolia and Thrace, broad-leaved deciduous mixed humid and pure, humid and coniferous stands are found (Satir, Berberoglu, & Cilek, 2016).

In the **Mediterranean** region (southern and western part) summers are hot and dry, while winters are mild and rainy. Mean annual temperature varies between 12°C and 20°C. The precipitation has a distinct seasonality (the number of dry months is about 3 to 4) and varies considerably from year to year, with mean annual ranging between 600 and 800 mm. This region represent a fire prone ecosystem characterized by sclerophyllous shrublands (mainly dominated by *Arbutus andrachne*, *Arbutus unedo*, *Calicotome villosa*, *Ceratonia siliqua*, *Quercus coccifera*, *Myrtus communis*, *Phillyrea latifolia*, *Pistacia terebinthus*, *Pistacia lentiscus*, *Spartium junceum*, *Styrax officinalis*), coniferous forests (*Pinus brutia*, *P. nigra*, *Cedrus libani*, *Abies cilicica*) and sub-alpine grasslands (Arca et al., 2012).

The **Iran-Turan** region (central and eastern part) is under the influence of continental climate. Mean annual temperature varies between 5° and 12° C and mean annual precipitation is less than

400 mm, except for the northeastern part of Eastern Anatolia. During the summer, in Inner Anatolia, there is a marked diurnal temperature change and drought is dominant all over the area. Rainfall maxima occur in spring months. The very low summer humidity is a major limiting factor for the vegetation. This favors a predominantly herbaceous flora and (with the exception of some conifers) the natural and anthropogenic steppes and dry forests of Central and Eastern Anatolia. The **Mesopotamian** region (south-eastern part) is the driest part of Turkey, with mean annual ranging between 15°C and 20°C (Sensoy et al., 2016). Relative humidity is around 30% in the major cities of Diyarbakir and Urfa, and can drop as low as 1%. The vegetation is characterized by the sparse steppes of arid southeastern Anatolia ((Ibrahim Atalay, Efe, & Öztürk, 2014), (Satir et al., 2016),(Ibrahim Atalay, 2016), (Ustaoglu & Aydinoglu, 2019)).

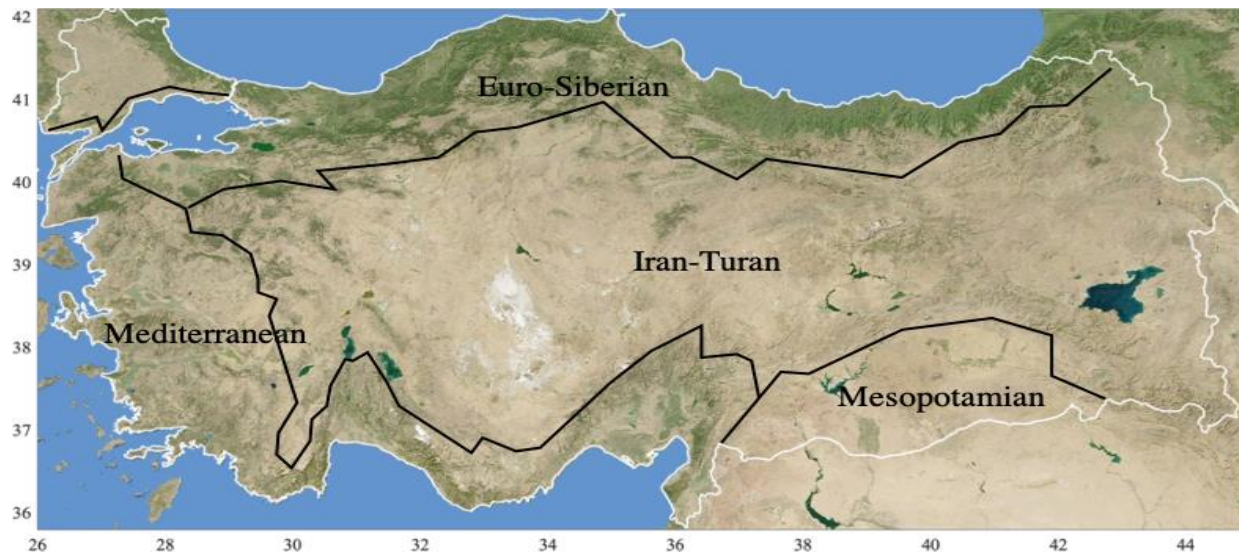


*Fig. 1. The four phytogeographical regions of Turkey: Euro-Siberian, Mediterranean, Iran-Turan and Mesopotamian (after (I. Atalay, 1986)).*

#### *Socio-economic features and their impact on the landscape*

Scientific and historical research indicates that 4,000 years ago the Anatolian landscape was 60% - 70% forests and 10%-15% steppes. Since then, over-grazing, over-cutting, fires, clearance for agriculture, wars and general misuse of the land have generated a completely different situation (Davis, 1970). Nowadays, 44% of the Country is covered by agricultural areas, steppes and scrub are around 22%, whereas forests, mainly covering the coastal and mountainous areas of the Mediterranean and Black sea region, represent only 15% of the total land area (Fig. 2).

Nearly 47% of forestland is constituted by coniferous species, more than 31% are broad-leaved whereas mixed coniferous and broad-leaved represent 22% of them (Fig. 3a).

In the *Steppes and Scrub* category, *Natural Grassland* represents 50% of the total, whereas the *Scrub* are mainly constituted by *Transitional woodland-scrub* (44%) with *Sclerophyllous vegetation* representing only 6% of the total (Fig. 3b).

55% of the *Agricultural areas* is represented by *Arable land* (Irrigated, Non-irrigated and Rice fields (Fig. 3d)), 33% is *Heterogenous Agricultural areas* (Annual crops associated with permanent crops, Complex cultivation patterns agriculture, with significant areas of natural vegetation, Agro-forestry areas), 6% is respectively *Pastures* and *Permanent Crops* (Vineyards, Fruit trees and berry plantations, Olive groves) (Fig. 3c).

After World War II radical socioeconomic changes occurred in North-Western Mediterranean countries that generated a strong migration from rural areas to urban centers. Land abandonment, together with afforestation programs, gradually resulted into a more fire prone landscape. In more recent years, this process has been further enhanced by a fast urban development with consequent expansion of the wildland-urban interface (Martínez-Fernández, Chuvieco, & Koutsias, 2013).

At the same time, in Southern and Eastern Mediterranean countries rural and forested area remained a primary resources for the subsistence of local communities, such that overgrazing, over-collection of fuel wood and clear-cutting continued to impose high pressure on forests. Nowadays, rapid population growth and development in some of these countries, such as Turkey, is changing this scenario (Merlo & Croitoru, 2005).

Over the past three decades, Turkey has experienced considerable population growth, from 56.4 million of 1990 (Ustaoglu & Aydinoglu, 2019), overpassing the 83 million at the end of 2019 (the 18<sup>th</sup> most populated country in the world), a 47.4% increase (Turkish Statistic Institute, 2020). This growth has been driven by a rapid economic development that speeded up consistently the urbanization process, such that nowadays around two-thirds of the population lives between the three largest cities (Istanbul, Ankara and Izmir) and other large and medium-size cities (Fig. 2). According to Corine Land Cover (CLC) maps, the *Urban Land Use* (Artificial areas) has increased by more than 60% from 1990 to 2018 (Tab. 1). This is mostly the result of migration to urban centers from rural areas, which have been losing population since the 1990s (Atmiş, Özden, & Lise, 2007).

In comparison to European counterparts, having more than 30% of its population living in rural areas (Ustaoglu & Aydinoglu, 2019), Turkey still holds a strong rural identity. Nevertheless, we are already witnessing the consequences of growing urban pressure on rural landscape through fragmentation of agricultural areas and woodland, while some landscapes are becoming more hazardous, due to augmented forest cover and closure. These processes seems to recall landscape dynamics we already witnessed in the northern and western European countries (Viedma, Moreno, Güngöroglu, Cosgun, & Kavgacı, 2017).

A recent study (Özşahin & Eroğlu, 2020) produced accurate maps of Turkey's anthrome classes showing anthropogenic pressures over the course of 25 years (1990-2015). The authors used the anthrome classification developed by the Anthromes Working Group (Ellis & Ramankutty, 2008) producing 500 x 500 m resolution maps through a comparative analysis of current research data and the dataset drawn from the National Land Cover Classification and Tracking System, validating them with LANDSAT and RASAT images.

The maps produced by that study show quite clearly a marked increase in the *Dense settlements* and *Villages* classes and a correspondent strong decrease in the Croplands class (Fig. 4a-b). Within this last category the *Residential croplands* (both *irrigated* and *rainfed*) have been growing in contrast to a halving of *Populated* and *Remote croplands* (Fig. 4c-d).

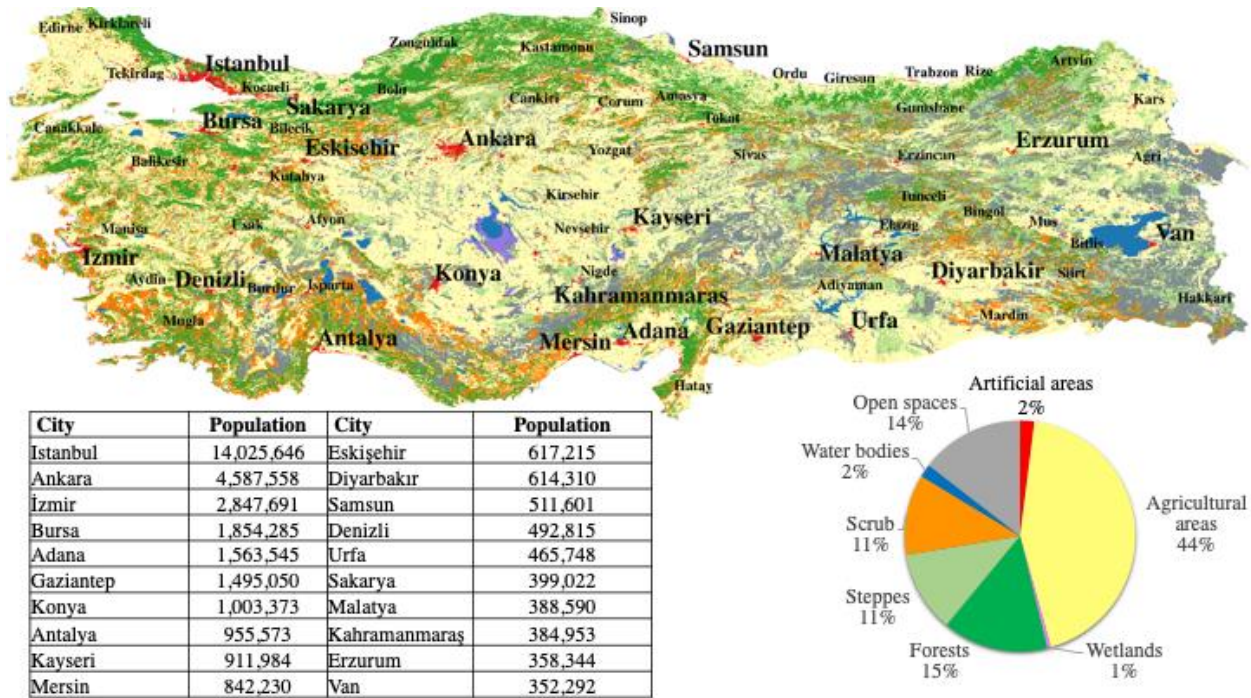


Fig. 2. Land use/cover classes (Label1) visualized with 100 m resolution (CLC 2018). In the table on the left, first 20 largest Turkish cities with their relative population (Turkish Statistic Institute, 2020).

CLC types	1990 (km2)	2018 (km2)	1990-2018 (%)
Artificial areas	9,591	15,592	62.57%
Agricultural areas	334,686	340,686	1.79%
Forests	116,813	115,210	-1.37%
Steppes	91,567	88,731	-3.10%
Scrub	87,151	88,187	1.19%
Open spaces	125,434	113,209	-9.75%
Wetlands	2,540	4,113	61.94%
Water bodies	11,991	14,052	17.19%

Tab. 1. Total surface of the main (Label1) land use/cover classes (km2) for 1990 and 2018, and the percentage of net change in land cover from 1990 to 201. (CLC 1990 and 2018).

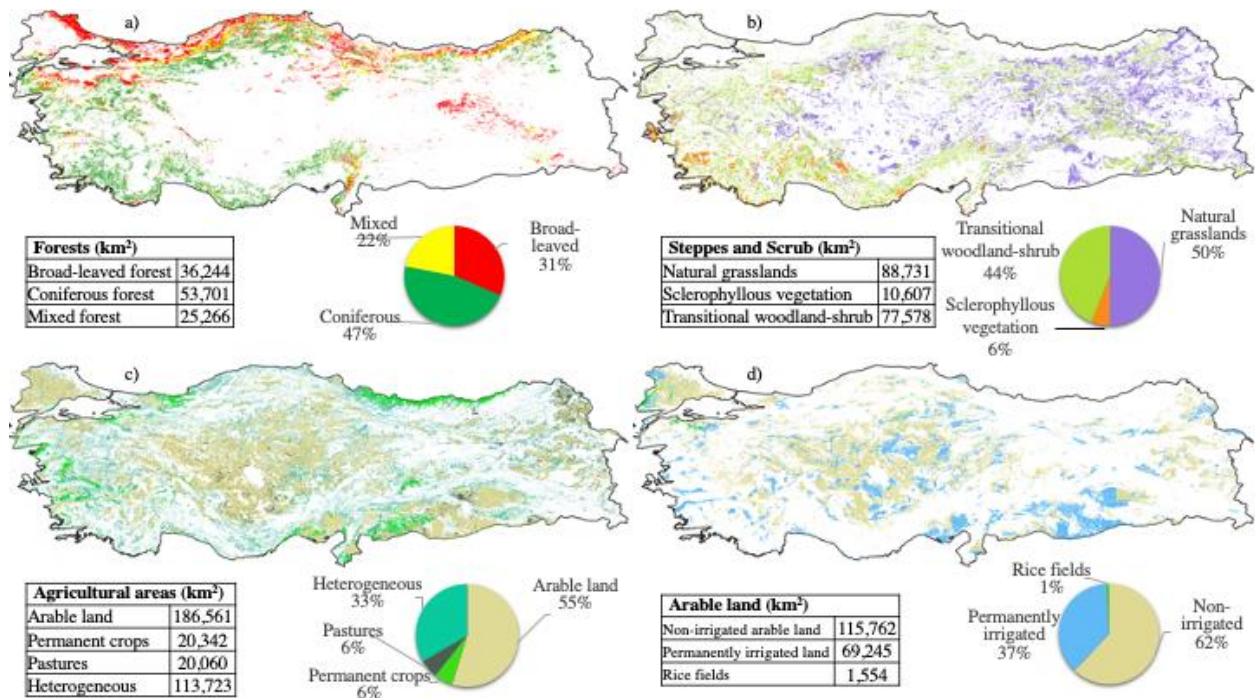


Fig. 3. (a) Forest types (Label3). (b) Steppes and Scrub types (Label3). (c) Agricultural area types (Label2). (d) Arable Land types (Label3). Visualized with 100 m resolution (CLC 2018).

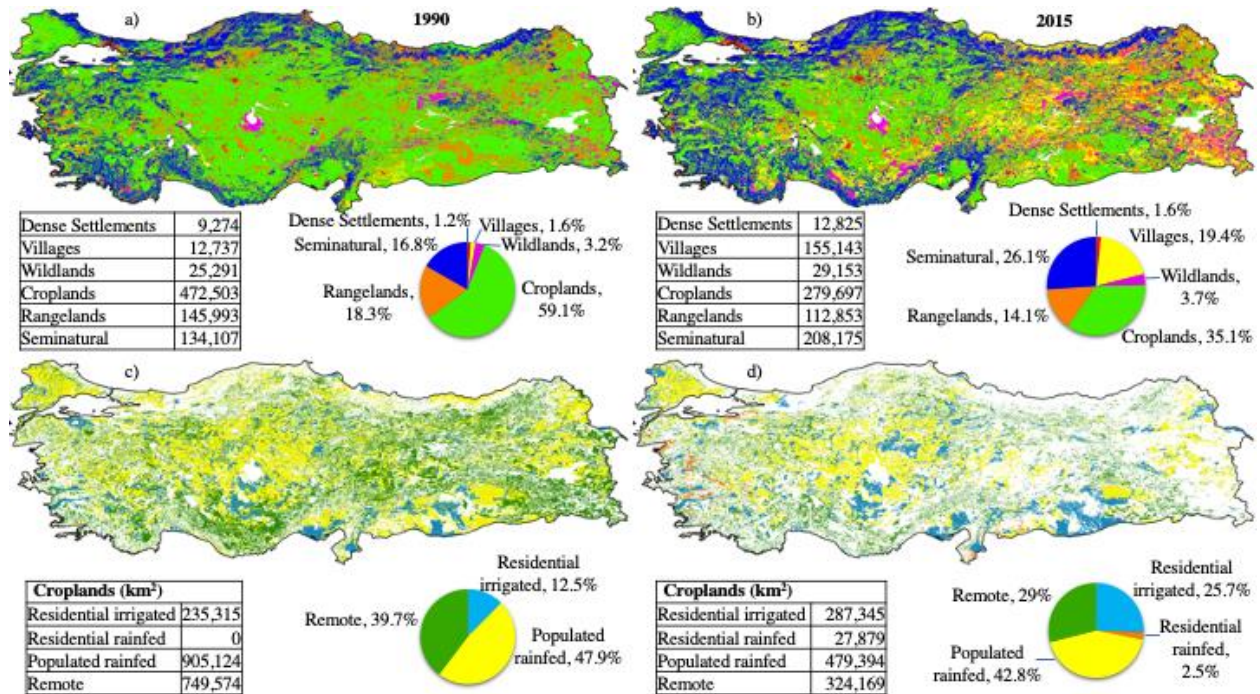


Fig. 4. Anthropogenic biomes in Turkey according to the Anthromes Working Group classification. (a) Aggregated classes (1990). (b) Aggregated classes (2015). (c) Croplands (1990). (d) Croplands (2015). Visualized with 500 m resolution (Özşahin & Eroğlu, 2020).

### *The geographical regions*

Turkey is a unitary state with three levels of government; the national level, 81 provinces and 1397 municipalities. (Ibrahim Atalay et al., 2014).

Another subdivision that can be useful to introduce is the one decided in 1941 in Ankara by the 1st Geography Congress, which identified 7 geographical regions:

- 4 coastal, named according to the 4 seas surrounding the Country: Black Sea, Marmara, Aegean and Mediterranean,
- 3 inner regions, whose name refers to their position inside the Anatolian peninsula: Central, Eastern and South Eastern (Organisation for Economic Co-operation and Development (OECD), 2017).

In Fig. 5a the geographical regions are depicted on a CLC (2018) map. If we combine this information with that discussed for Figure 1, it is easy to understand that these regions were chosen because of their quite distinct characteristics in terms of climate, flora and fauna, human habitat, agricultural diversities, etc. In fact, Black Sea and northern Marmara region belong to the Euro-Siberian phytogeographical region, southern Marmara, Aegean and Mediterranean belong to the Mediterranean region, Central and East Anatolia occupy almost entirely the Iran-Turan region whereas South Eastern Anatolia is basically the Mesopotamian region.

Apart from their phytogeographical features, that we described above while discussing Fig. 1, from Fig. 5 we can say something on the human impact in shaping the landscape of these regions during the course of the time.

The first thing we notice is that *Agricultural areas* is the main land cover in all of them, but is really predominant (more than 50%) in Central and South East Anatolia and in Marmara region (in the last case, mostly due to the contribution of the Thracian part). According to recent studies, “cereals represent nearly two-thirds of the harvested land in Turkey, most notably wheat (35%), barley (12%), and maize (10%). Additionally, sugar beets (25%), potatoes (7%), sunflower (3%), cotton (3%), and pulses (2%) are grown (Rufin et al., 2019).

*Forests* rank as second main land cover in the Black Sea and Marmara regions (36% and 29% respectively), the most humid part of Turkey. In the Aegean and Mediterranean regions it becomes the third main land cover (around 20%), right after *Scrub* (that in the CLC classification combines sclerophyllous vegetation and transitional woodland shrub), mainly due to the specific feature of the Mediterranean climate, discussed above.

Just to understand how the coastal regions differ from the inland regions, *Forests* is only the 5th most extensive land cover type (always less than 5%) in this part of Turkey, following *Open spaces* (more than 30% of the territory in East Anatolia region), *Steppes* (more than 20% of the territory in the East Anatolia), and *Scrub*.

Apart from the fact that often information about fires are available aggregated at this level of country division, these 7 regions, can help to fast visualize the main environmental and anthropogenic features of Turkey, that can facilitate our future discussion about spatial distribution and characteristics of biomass burnings.

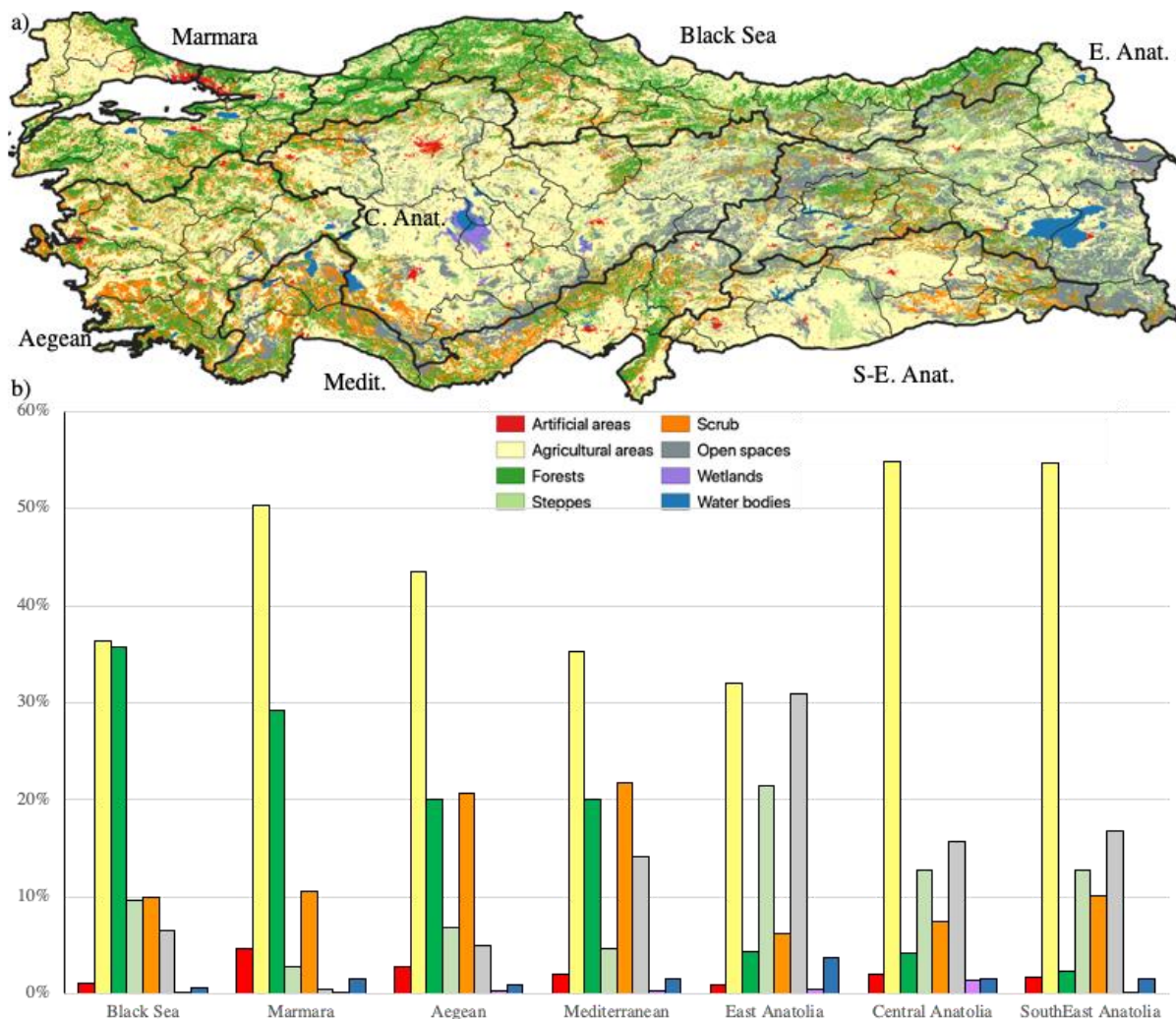


Fig. 5. (a) The 7 geographical regions of Turkey and the 81 provinces on Land use/cover classes visualized with 100 m resolution. (b) Percentage of the land cover/use classes in each geographical region. (CLC 2018)

## 2.2 Fire issues in Turkey

In Turkey, as for the majority of the countries, historical information about fires have been primarily related to wildfires, which are those reported by forest agencies on the provincial and regional level (many times difficult to obtain and often not digitized).

From the European Forest Fire Information System (EFFIS) fuel map (European Forest Fire Information System (EFFIS), 2017) in Fig. 6, we can see how most of the fuel vegetation with the potential of sustain large burnings (*Shrub* and *Timber* fuel categories) is located between the Black sea and the Mediterranean coastal regions, while Central, East and South-East Anatolia are characterized mostly by *Grass* fuel category.

The forestlands with highest density are located in the Black Sea region which, differently from the Mediterranean coast, dominated by conifer forestlands, has a strong presence of largely deciduous stands (see Fig. 3a). Here is possible to recognize two fire seasons :

- in Spring, before leaf-out, when the last year's surface fuels are dried up before the new vegetation period starts.
- in Autumn, after the vegetation period has ended and leaves fallen.

In both cases the burnings spread basically on the surface since this is the only layer with fuel available for the combustion. (Bekar & Tavşanoğlu, 2017).

According to official records, 41% of the fires occur in Aegean, 24% in Mediterranean, 22% in Marmara, and 13% in other regions (Ozturk, Gucel, Kucuk, & Sakcali, 2010).

If we refer to South Marmara, Aegean and Mediterranean regions as Mediterranean Turkey, considering what we discussed in the previous paragraph about the environmental and anthropogenic features of this part of the country, it is not a surprise that almost all the available studies on this topic are focus here. In fact, approximately 57% (12.5 millions ha) of Turkey's forest area is located in this high fire sensitive region.

Long-lasting periods with hot and dry weather in summer, combined with warm and rainy winters and a long history of human modification, including the use of fires to transform naturally vegetated areas into pasture and croplands, shaped the fire regime. It is characterized by “very little winter activity, followed by an increase in May as the rain activity decreases and fuels start to dry up, a peak in the number of fire starts in August, followed by decreasing activity in the fall” (European Commission, 2018).

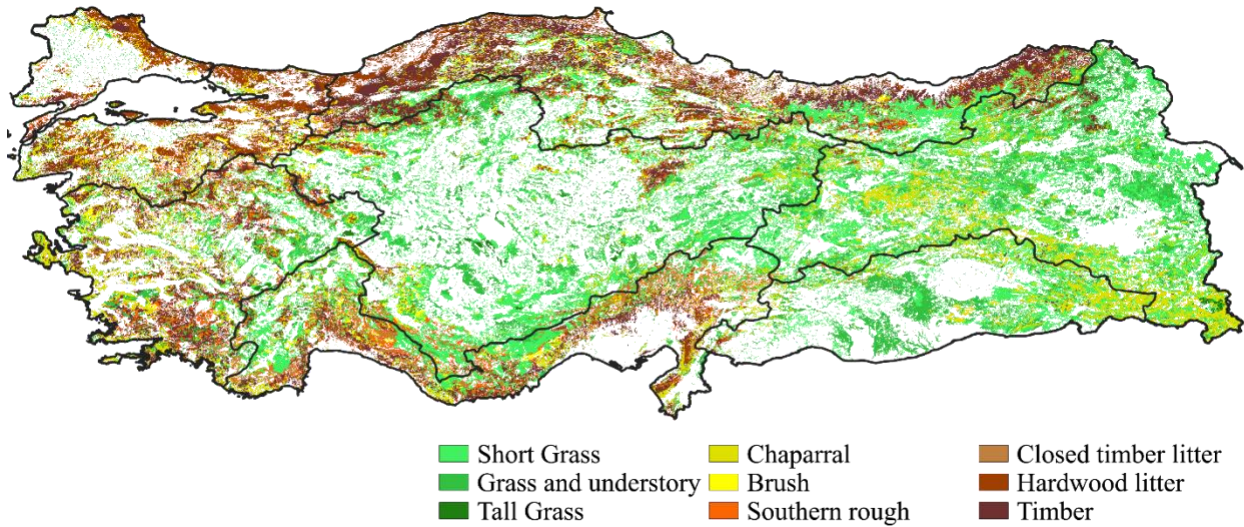


*Fig. 6. The EFFIS fuel map. Fuel categories of the Northern Forest Fire Laboratory (NFFL) or fire behavior models (Anderson, 1982).*

### 2.3 Satellite Data

Satellite instruments can detect either the thermal emission during a fire, or the burnt area after. The latter are known as ‘burnt area’, ‘burnt scar’, ‘burnt pixel’ or ‘fire affected area’, while the first products are referred to as ‘hot spots’, ‘active fires’, ‘fire pixels’ or ‘fire counts’ ((Kaiser et al., 2009), (Roy, Boschetti, & Smith, 2013), (Pereira et al., 1999)).

Active fire detection from satellites takes advantage of the fact that as target temperature increases radiance increases faster at the shortwave end of the spectrum when compared to the long-wave end. By using two atmospheric window spectral channels, such as the 3.9 and 11  $\mu\text{m}$ , fire locations and characteristics can be determined (Kaiser et al., 2009).

Active fire products provide the detection time and location of a hot spot and other important parameters with a view to obtain relevant information on the detected hot spot.

For long time, characterization of active fires from space were obtained from existing satellite observations retrieved with sensors developed for other purposes. The appearance of the Moderate Resolution Imaging Spectroradiometer MODIS sensor (in 1999 and 2002 on board of Terra and Aqua satellites respectively) meant a significant step forward. In fact, from its beginning the 3.9  $\mu\text{m}$  bands on the MODIS instrument were designed with fire detection in mind. And, at this

moment, the MODIS Active Fire Products are one of the most consolidated and a reference for global Earth observation of biomass burning (Dozier, 1981).

The MODIS Active Fire Products detect flame fronts in 1km pixel at the time of the satellite overpass, under relatively cloud-free conditions, that are warm enough to be detected by the respective contextual algorithms. The thresholds are first applied to the observed middle–infrared (MIR) and thermal infrared (TIR) brightness temperature and then false detections are rejected by examining the brightness temperature relative to neighboring pixels (Giglio, Schroeder, Hall, & Justice, 2018).

Fire scar detection is based on rapid drops in vegetation-related reflectance of the area affected by the fire burnings associated with the charring and removal of vegetation. While the increased soil exposure and radiation absorption by charred vegetation, and decreased evapotranspiration relative to the pre-fire green vegetation, produces a rise in shortwave infrared reflectance and brightness temperature ((Giglio, Descloitres, Justice, & Kaufman, n.d.), (Pereira et al., 1999)).

Active fire data from the latest MODIS fire product (MCD14ML, collection 6) were collected from March 2003 to December 2019. Together with location and timing of active fires at native resolution (1 km at nadir) for the MODIS Terra and Aqua satellites, this dataset reports its MIR and TIR brightness temperatures, detection confidence and the Fire Radiative Power (FRP)<sup>1</sup>(Lentile et al., 2006). The latter was used to visualize the dataset in Fig. 7a (the Jenks natural breaks method (JENKS & F., 1967) is used to segment continuous data).

The 81 Turkish provinces were selected as spatial units to carry out the analysis. The units where there were less than 170 active fire counts for the entire study period (an average of less than 10 per year) were removed, to ensure reliable statistical analysis. As a result, the final number of units is 65. The provinces removed belong to the Black Sea region, characterized by cold and humid climate, and to the barren or sparsely vegetated lands of the most Eastern part of the Country (see Fig. 5). A complete list of the 81 Turkish provinces together with their identification number and the number of MODIS active fires for the entire study period is provided in Appendix A (Fig.A 1 and Tab.A 1).

---

<sup>1</sup> Fire Radiative Power (FRP) is a measure of the radiant energy liberated per unit time from burning vegetation via the rapid oxidation of fuel carbon and hydrogen. It has been demonstrated in small-scale experiments that this parameter, is related to the rate at which the fuel biomass is being consumed (Heward et al., 2013).

The MCD64A1 Burned Area Product is a monthly product containing per-pixel (500 m) burning and quality information, and tile-level metadata. The product algorithm ultimately identifies the burn dates in ordinal day format (Giglio et al., 2018). Turkey is embedded between tiles 8 and 15 of the 24  $10^{\circ} \times 10^{\circ}$  tiles that cover almost the entire land mass. The monthly burn date maps for these two tiles for the same time span were collected in shapefile format, merged together, and filtered over the selected units of the study area (Fig. 7b).

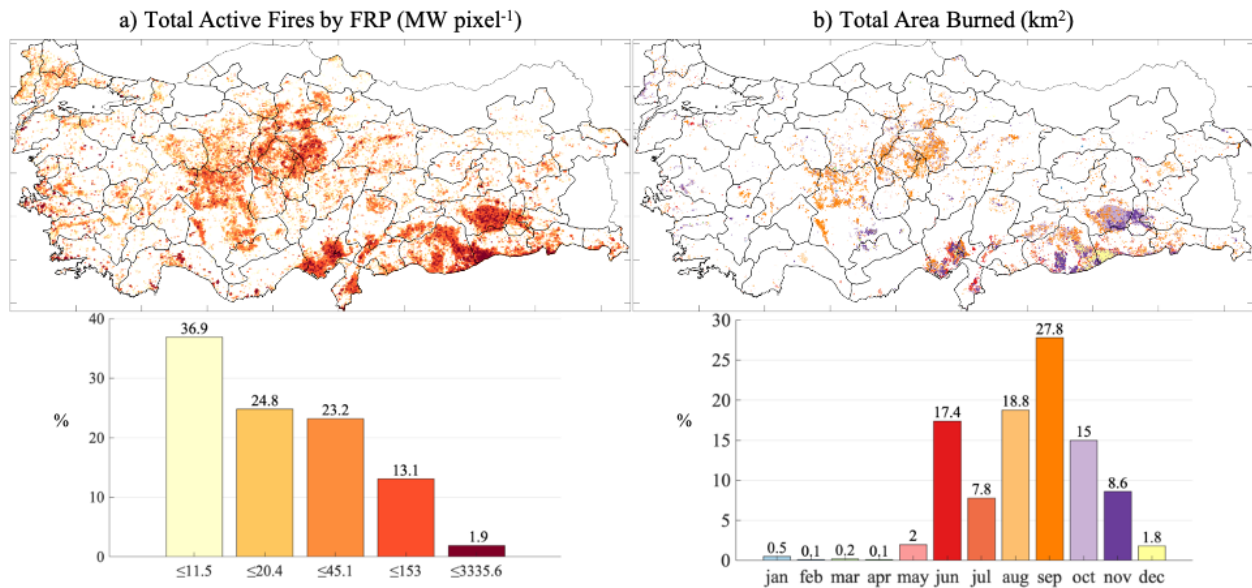


Fig. 7. MODIS active fires (2003-2019) ordered by FRP (a). MODIS burned area (2003-2019) ordered by the month of the year it was detected (b). Below the percentage referring to the classes identified by respective colors.

## 2.4 Fire Regime variables

Eleven variables were computed to describe the *sensu stricto* and *sensu lato* characterization of the fire regimes in each of the selected unit of the study area.

The *sensu stricto* characterization describes spatial (fire incidence and fire size distribution), temporal (interannual variability, season length, season modality and percentage of peak months occurring in summer) and intensity (fire intensity) characteristics of the fire activity. Whereas the *sensu lato* (Giglio, Boschetti, Roy, Hoffmann, & Humber, 2016) assists with fire regime interpretation, representing key antecedent conditions, which will be represented by anthromes

(Ellis & Ramankutty, 2008) and Köppen climate classes (Kottek, Grieser, Beck, Rudolf, & Rubel, 2006).

### *Sensu Stricto characterization*

The total number of MODIS active fire counts/pixels (Fig. 8a) and the total burned area (Fig. 8b), in each unit for the entire study period, have been used to define the fire **Incidence, IC** (Krebs, Pezzatti, Mazzoleni, Talbot, & Conedera, 2010). The Jenks natural breaks method was selected to segment continuous data for mapping all quantitative variables.

Regularity of fire occurrence for each unit has been evaluated by calculating the interannual coefficient of variation (CoV, standard deviation ( $\sigma$ ) divided the mean value ( $\mu$ )) of total number of active fire pixels and total burned area (Andela et al., 2019, Chen et al., 2017). This parameter defines the **Interannual variability, VT** (dimensionless). Low values of this variable indicate regular fire occurrence whereas high values represent sporadic fire occurrence (Fig. 8c-d).

Fig. 9 shows the temporal behavior of the active fires. The variables **Season Length, SL** (months) and **Season modality, MT** (dimensionless) for each unit have been defined with a novel methodology described in details in Appendix B.

For each unit, we calculate the month with the highest number of active fire pixels recorded by MODIS for each year of the study period, in order to determine the percentage of fire peak months belonging to the summer period (June to September). With this, we compute the variable **Percentage of Summer Peak Month, PSPM** (Fig. 9c). Together with this, we also mapped the month with the most active fire pixels recorded by MODIS during the 17 years of the study period (Fig. 9d).

As mentioned before, one of the parameters provided from the MCD14ML product for each active fire detection is the Fire Radiative Power (FRP). It measures the radiant energy released per unit time from burning vegetation via the rapid oxidation of fuel carbon and hydrogen (Cox, 2016) and provides the best information of fire line intensity at the time of satellite observation. Due to the skewed nature of the FRP distribution (Wooster, Zhukov, & Oertel, 2003) the most effective metric to help distinguish between fire types and regimes is the 90th percentile of FRP (Oliveira, Maier, Pereira, & Russell-Smith, 2015). In order to address this, we defined the variable

**Intensity, IT** (MW pixel-1) as 90th percentile of fire radiative power values recorded in each unit for the entire study period (Fig. 9e).

A complete list of the sensu stricto variables with their description is available in Tab. 2.

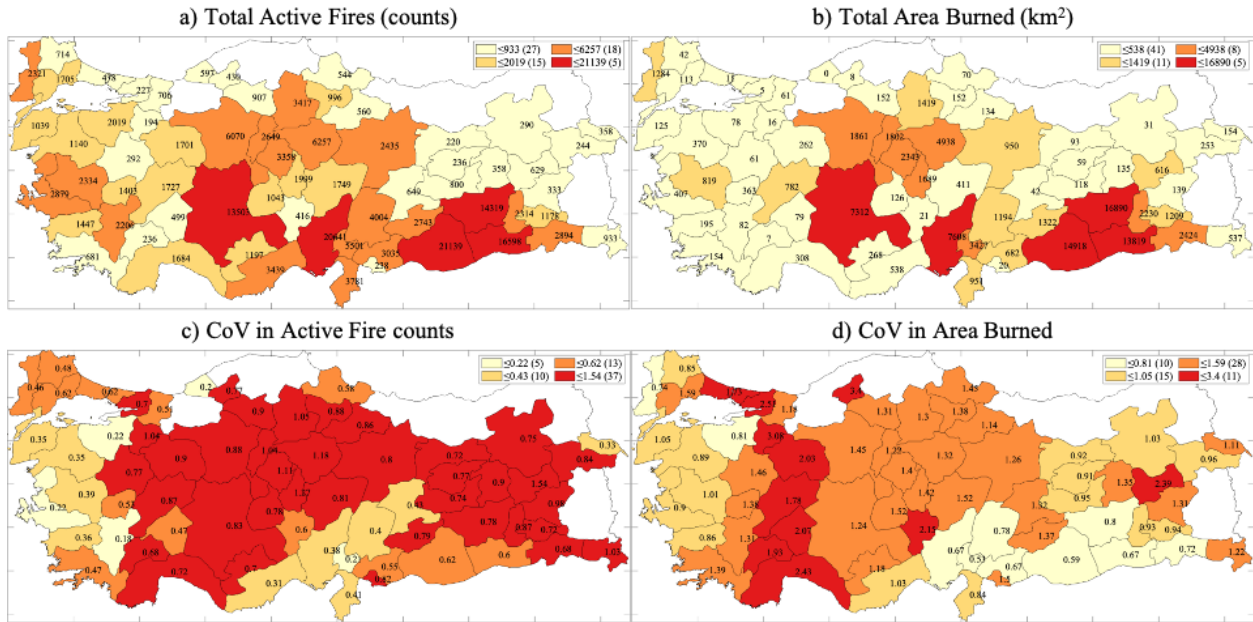


Fig. 8. Maps of fire incidence (a, b) and its inter-annual variability (c, d) in Turkey based on MODIS active fire data (a, c) and burned area data (b, d).

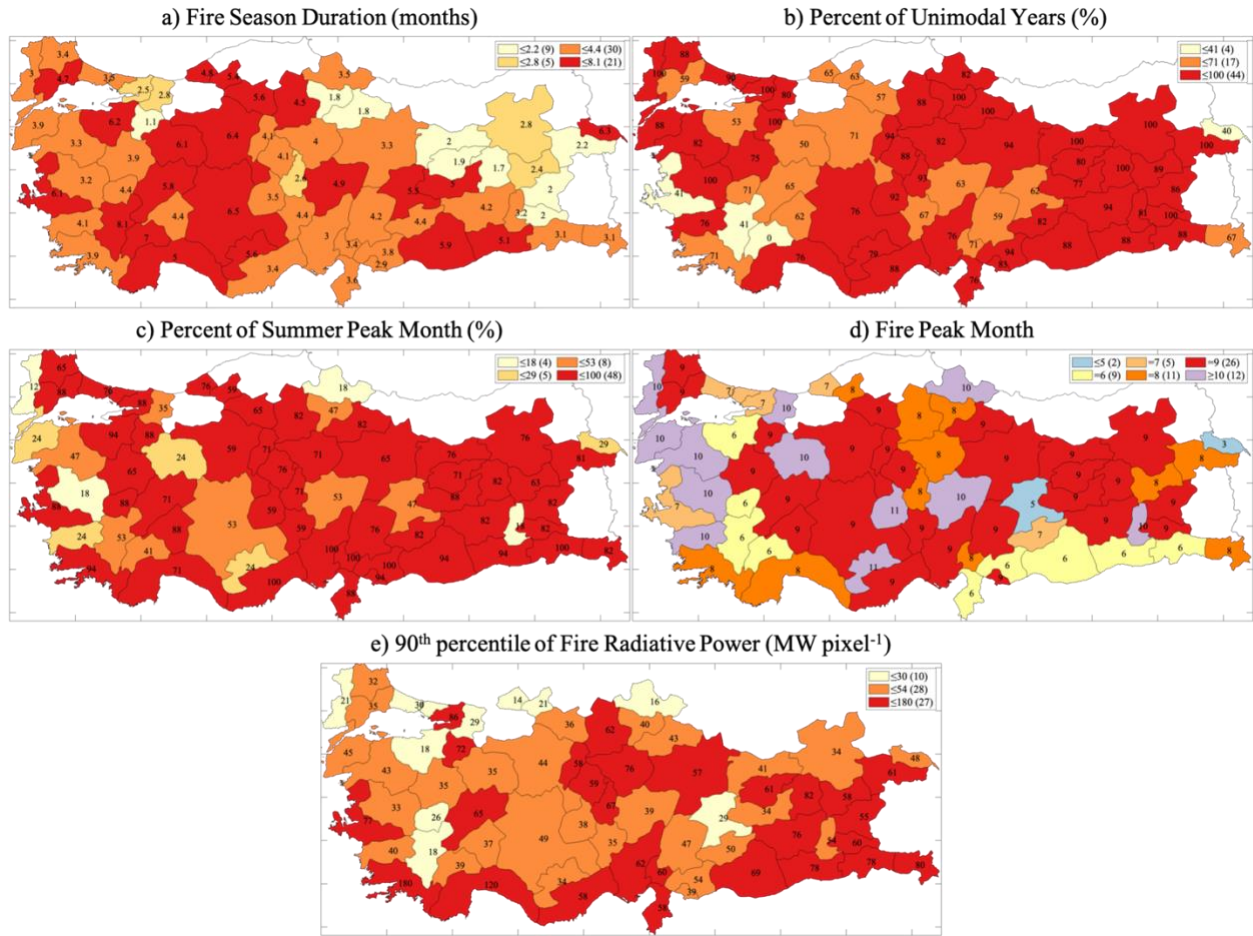


Fig. 9. Maps of fire season duration (a), fire season modality (b), and percentage of yearly fire peak month that belong to the summer period (June to September) (c), fire peak month (d), and fire intensity (e) in Turkey based on MODIS active fire data.

No.	Category	Abbr.	Variable	Units
1	Incidence Active Fires	ICAF	Total number of active fires	counts
2	Interannual variability Active Fires	CVAF	Inter-annual CoV in annual active fires	[]
3	Incidence Area Burned	ICAB	Total burned area	km <sup>2</sup>
4	Interannual variability Area Burned	CVAB	Inter-annual CoV in annual Area Burned	[]
5	Season Length	SL	Fire Season Duration	days
6	Season modality	MT	Percent of Unimodal Years	[]
7	Percentage of Summer Peak Month	PSPM	Percentage of Summer Peak Month	[]
8	Intensity	IT	90 <sup>th</sup> percentile of FRP	MW pixel <sup>-1</sup>

Tab. 2. List of *sensu strictu* variables: CoV = Coefficient of Variance.

### *Sensu lato* characterization

Turkey landscape is a result of a deep transformation by different civilizations on the natural biomes, since the beginning of the history. In light of this, the need of an accurate description of

human produced ecological patterns is particularly relevant for our study area. We downloaded the Anthromes 12K dataset (Ellis, Beusen, & Goldewijk, 2020), representing the most recent version of the maps of the Anthropogenic Biomes of the World produced by the Anthromes Working Group and compared it to the adapted maps described in (Özşahin & Eroğlu, 2020), introduced previously.

The Anthromes 12K is a global scale dataset at 5' (ca. 8 km at the Turkish latitudes) spatial resolution, while the maps produced by Özşahin & Eroğlu (2020) have a resolution of 500 m and are the result of an accurate work of adaptation of the classes defined by Anthromes Working Group to the Turkish territory. Fig. 10a-b show the differences between these two products for the year 2015 and with regard to the six aggregated classes of the Anthromes 12K: Dense settlements, Villages, Croplands, Rangelands, Forested lands, and Wildlands. While the global dataset tends to assign the category Croplands to large part of the Country, the adapted one detects the presence of Rangelands areas in East Anatolia, where livestock activities are common as visible in the national economic statistics.

When looking only at the cropland class, we notice even larger differences between these two datasets (Fig. 10c-d). According to Antomes 12K map for the year 2015 rainfed croplands with substantial human presence (Residential rainfed) is by far the most common in Turkey. On the contrary, this category is very marginal in the adapted map where rainfed croplands with significant human presence (Populated rainfed) is the most populated class with a relevant presence of Remote croplands (derisory in the global map) and Residential irrigated (with this category showing the largest agreement with the Corine Land Cover map 2018 (see Fig. 3d). For the scope of this work, the Turkish adapted map is more appropriate to describe the antecedent qualitative variable **Anthromes** (nominal). In Fig. 11 we used this map relative to the aggregated anthromes to summarize the land cover composition in each province, either as dominant anthrome or as combination of the two most extensive ones when the difference between the first and second most extensive type is less than 10%. Fig. 12 shows the same map but this time with the cropland types instead.

The second antecedent variable used in the sensu lato analysis is **Köppen climate classification** (nominal), based the on most common climate classification: the Köppen-Geiger (Kottek et al., 2006). This considers five main climate groups (A: Tropical, B: Arid, C: Warm

temperate, D: Cold, E: Polar), divided into 14 climate types, with classification criteria based on patterns of seasonal precipitation and temperature.

For this study, the Köppen climate classes map of Turkey produced by (Yılmaz & Çiçek, 2018) and available online (Yılmaz & Çiçek, n.d.) was used. According to the authors of this adapted map the global maps available “cannot reflect the diversity in Turkey in the exact manner due to the lack of data and scale problem” (Yılmaz & Çiçek, 2018). This map is based on a comparison between average temperature and precipitation from 249 meteorological stations located in Turkey and model data (Hijmans, Cameron, Parra, Jones, & Jarvis, 2005).

Four out of five of the main climate groups (B, C, D and E) are present in Turkey and there is no site belonging to the tropical climate zone (A). For the scope of the study, we reduced the detail of classification of the adapted map to the second level of the Köppen classification scheme, and considered only one class for the *Arid* climate (B), and merged the marginal *Polar Tundra* type (ET) with the *Cold* group (D) (Fig. 13).

The Mediterranean Turkey and the Southeast Anatolian region are characterized by *Temperate, dry summer* (Cs) climate type.

Apart from the region of Konya, revealed to be *Arid* (B), together with a small area in the southern of the Southeast Anatolia, the plateau of Central and East Anatolia are generally covered by *Cold, dry summer* (Ds) type.

The Black Sea coast and the regions in the inlands affected by the presence of the sea show climate types *Temperate, w/out dry season* (Cf). The North East corner of Anatolia (the Erzurum-Kars region) and the Ilgaz-Kure mountainside are characterized by *Cold, w/out dry season* (Df) climate. Based on the map just described, in Fig. 14 we summarized the climate composition in each province, either as dominant climate type or as combination of two most extensive ones when the difference between the first and second most present types was less than 30%.

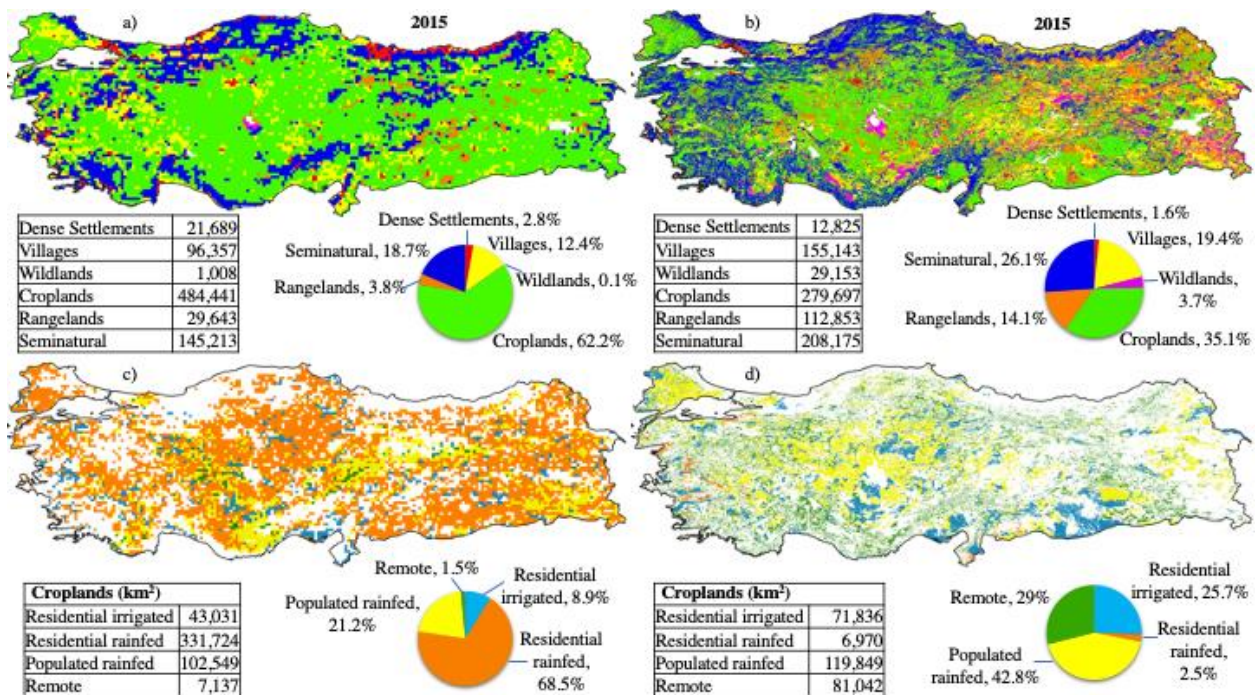


Fig. 10. Anthropogenic biomes in Turkey according to the Anthromes Working Group classification. (a) Anthromes 12K map of 2015 - Aggregated classes. (b) Adapted map of 2015 - Aggregated classes (2015). (c) Anthromes 12K map of 2015 - Croplands. (d) Adapted map of 2015 - Croplands). Anthromes 12K maps are visualized with 5' (ca. 8km) resolution while the Adapted maps are visualized with 500 m resolution.

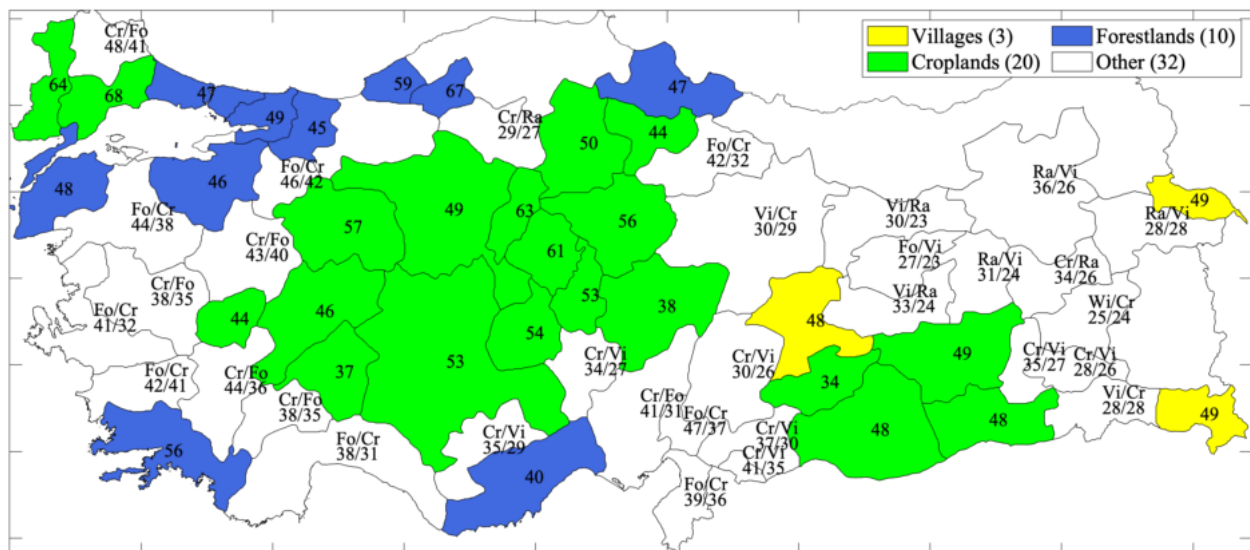


Fig. 11. Map of the dominant Anthromes (Aggregated classes) for each provinces (%), based on the adapted map for 2015 (Özşahin & Eroğlu, 2020). When the difference between the 1<sup>st</sup> and 2<sup>nd</sup> most extensive Anthrome is less than 10% both classes are reported with their relative percentage (%) under the category “Other” in white. (Vi: Villages; Wi: Wildlands; Cr: Croplands; Ra: Rangelands; Fo: Forests).

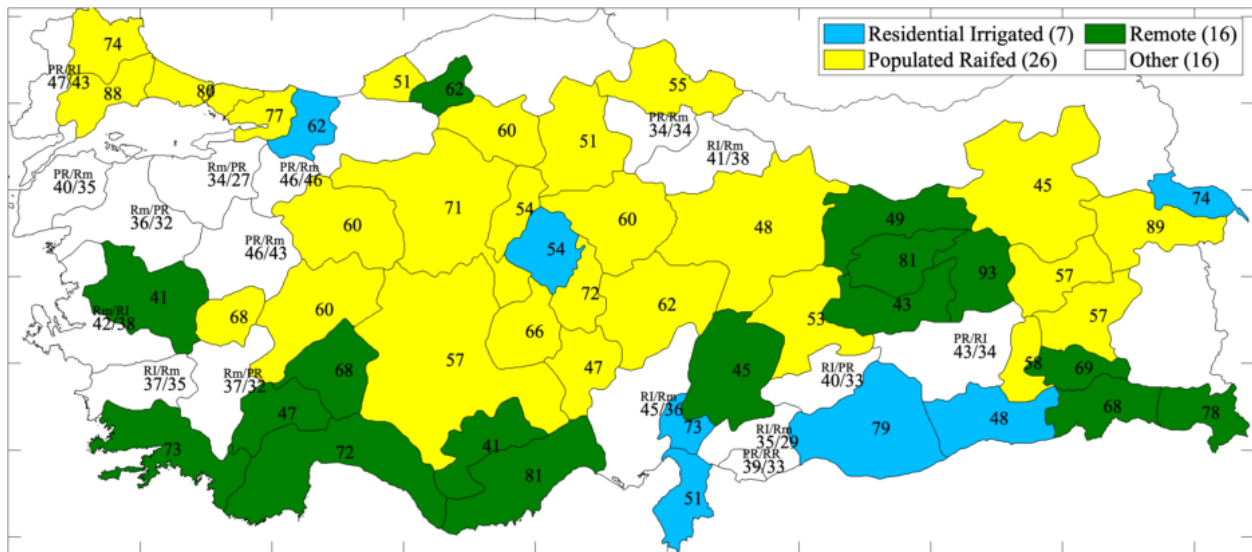


Fig. 12. Map of the dominant Cropland types for each provinces (%), based on the adapted map for 2015 (Özşahin & Eroğlu, 2020). When the difference between the 1<sup>st</sup> and 2<sup>nd</sup> most extensive type is less than 10% both classes are reported with their relative percent (%) under the category “Other” in white. (RI: Residential Irrigated; RR: Residential Rainfed; PR: Populated Rainfed; Rm: Remote).

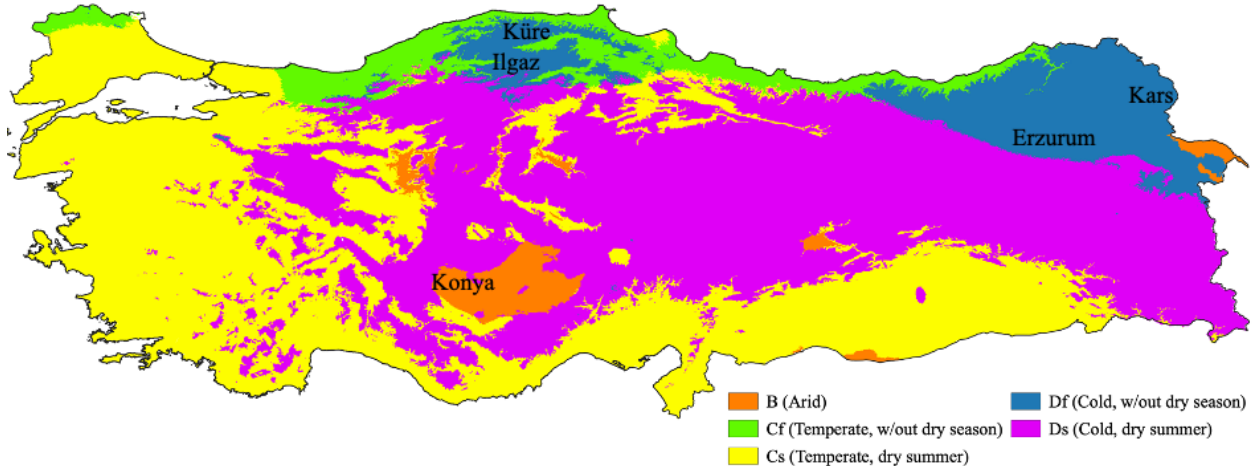


Fig. 13. Köppen climate types of Turkey. Adapted map visualized with 1 km resolution (Yılmaz & Çiçek, n.d.). (B: Arid; Cf: Temperate, w/out dry summer; Cs: Temperate, dry summer; Df: Cold, w/out dry summer; Ds: Cold, dry summer ).

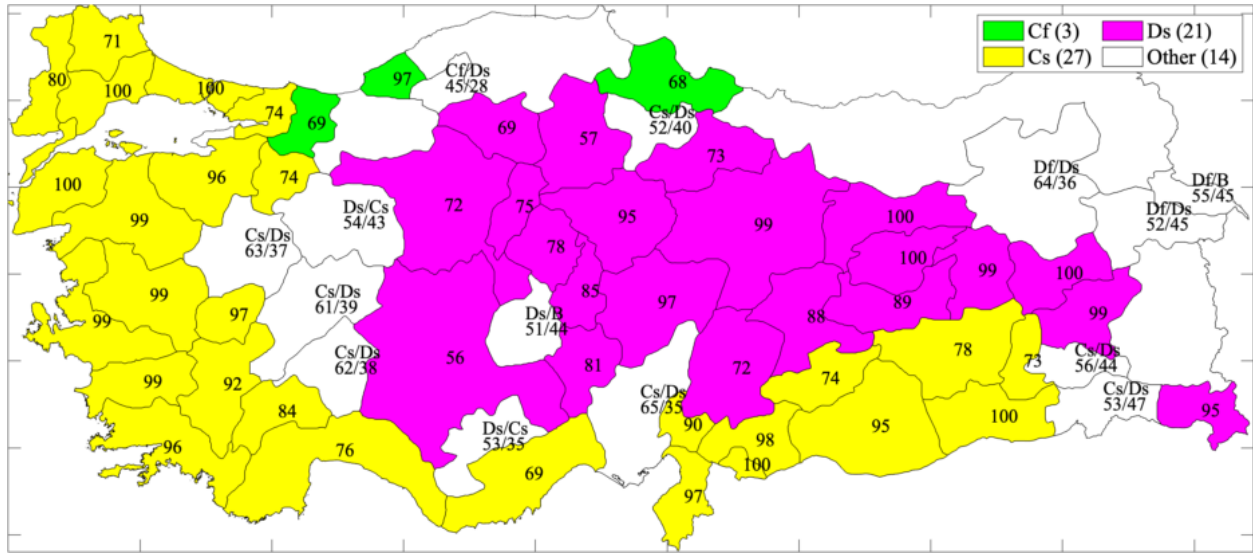


Fig. 14. Map of the dominant Climate types for each provinces (%), based on the adapted map (Yılmaz & Çiçek, n.d.). When the difference between the 1st and 2nd most extensive Climate type is less than 30% both types are reported with their relative percent (%) under the category “Other” in white.

## 2.5 Description of the spatial patterns of the MODIS data

### *Sensu stricto*

Fig. 8 shows fire incidence and its inter-annual variability. Both, the map of total active fire counts (Fig. 8a) and burned area (Fig. 8b) show that the most fire prone provinces are located in Southeastern Turkey (Sanliurfa, Mardin, Diyarbakir; see Appendix A Fig.A 1 and Tab.A 1 for a map of Turkey with province names), Central Anatolia (Konya, Yozgat, Ankara), and Southeastern part of the Mediterranean Turkey (Adana, Osmaniye, K. Maras). The map of active fires describes a more intense fire activity in the West Mediterranean Turkey with respect to what is shown by burned area data.

From Fig. 8c-d is possible to observe that area burned data have a higher range of variability (0.53 – 3.4) compared to active fire data (0.18 – 1.54). This difference plays a part in the fact that the two maps look different in terms of relative variability between the different provinces. In fact, despite having similar values of CoV, the Southeastern provinces of Turkey, with high fire incidence, have higher relative variability in the active fire map than in the burned area one. Both maps show higher variability of inter-annual fire activity in the Central Anatolian provinces, and they both agree regarding the lower variability of the Southeastern and Western provinces of Mediterranean Turkey.

The fire season duration is higher, generally between 5 and 6 months, in the Central Western and in the highly fire active provinces of Southeastern Turkey. While it ranges between 3 and 4 months for the rest for the country, with the exception of the Northern Eastern provinces where it is usually confined between 2 months.

The fire seasons are mainly unimodal all over the country, with a percentage of unimodal years during the study period exceeding the 50% for all the Turkish provinces, with the exception of few provinces spotted in the Aegean region and one in East Anatolia.

A similar behavior we can observe for the fire peak months, occurring mainly in the summer for most of the provinces, with the exception of eight provinces concentrated between the Aegean and Marmara regions, and five more provinces spotted in the rest of the country

The peak month during the whole study period occurred primarily at the beginning of summer in Southeastern Turkey and in the end of summer in Central Anatolia and Southeastern provinces of Mediterranean Turkey and in autumn in the Western provinces of this last region (Fig. 9).

The highest fire radiative power is detected in the Southern Mediterranean provinces of Mugla (180 MW pixel<sup>-1</sup>) and Antalya (120 MW pixel<sup>-1</sup>), reach of forests. High values are also recorded in the *residential irrigated croplands* of Southeastern Anatolia and Southeastern Mediterranean Turkey and in the *rangelands* of East Anatolia, while lower values are seen in the *populated rainfed croplands* of Central Anatolia (Fig. 9e).

#### *Sensu lato*

Fig. 15 gives an overview of the distribution of the active fires in the main classes of the auxiliary variables: anthrome and climate types.

Despite occupying only 35.1% of the study area (Fig. 10b), *Croplands* (Cr) is the anthrome where 74.5% of the reported active fires were detected. Within this category 65.8% of them have been located in the sub-category *Residential Irrigated* (RI) accounting only for 25.7% of this anthrome. Almost all of the remaining active fires (31.1%) have been reported in the sub-category *Populated Rainfed* (PR), accounting for 42.8% of the cropland anthrome.

Regarding the Climate variable, 74.2% of the active fires were detected under *Temperate, dry summer* (Cs) climate type (covering 39.4% of the study area), while 20.2% of the remaining ones belong to *Cold, dry summer* (Ds) type (accounting for 43% of the study area).

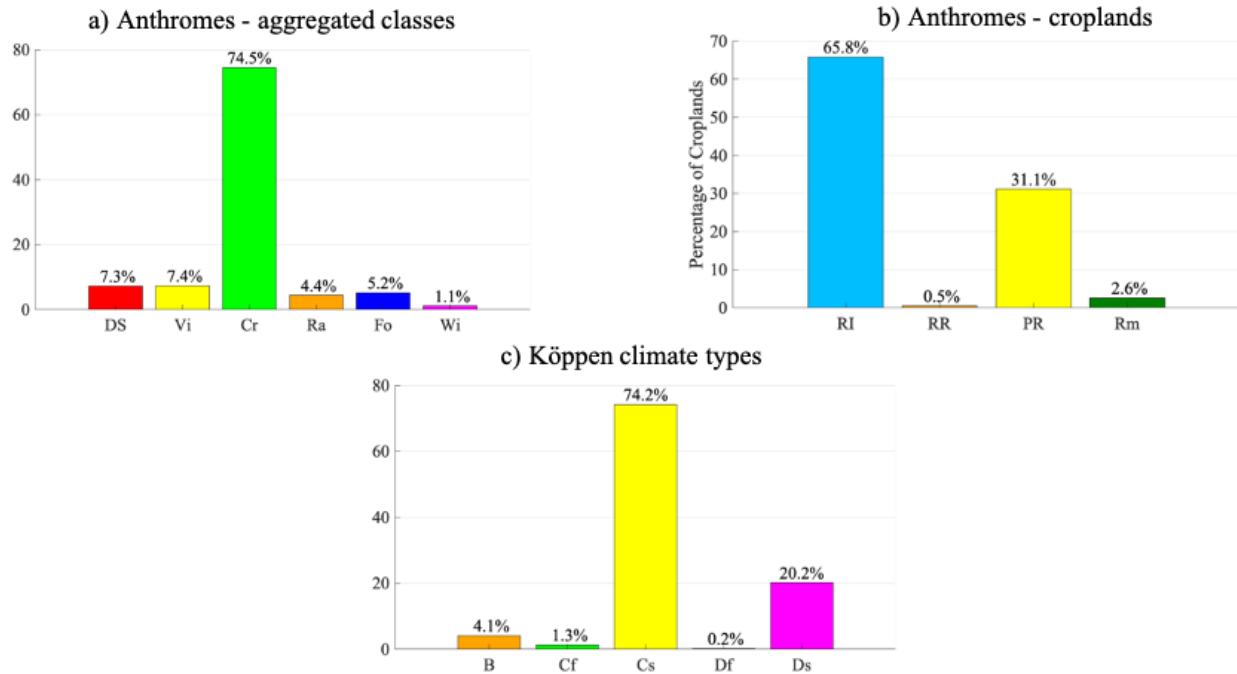


*Fig. 15. MODIS active fires (2003-2019) ordered by Anthromes – Aggregated classes (a), Anthromes – Croplands (b) and by Köppen climate types (c). (Vi: Villages; Wi: Wildlands; Cr: Croplands; Ra: Rangelands; Fo: Forests). (RI: Residential Irrigated; RR: Residential Rainfed; PR: Populated Rainfed; Rm: Remote). (B: Arid; Cf: Temperate, w/out dry summer; Cs: Temperate, dry summer; Df: Cold, w/out dry summer; Ds: Cold, dry summer )*

## 2.6 Principal Component Analysis (PCA)

In the previous paragraphs we presented the eight quantitative variables that describe spatial temporal and intensity aspects of the fire regime in the 65 selected provinces.

Due to the large number of variables, it is hard to describe all of the relationships between them without reducing the data dimensionality and select just the top few features that satisfactorily represent the variability of the dataset. The PCA is a data reduction technique that allows to do this reduction whilst retaining as much of the variability in the data as possible. It does it by creating a new set of synthetic variables called principal components (PC) or factors. The first PC is a linear combination of the (standardized) original variables and explains as much variability as possible of the overall data variability. Each subsequent component explains as much as possible of the remaining variability, under the condition that it is uncorrelated with the previous components.

Starting from our original numerical dataset structured in 65 observations / 8 quantitative variables (see Tab. C 1 in Appendix C for the complete data-set). It allows to:

- Quickly visualize and analyze correlations between the 8 variables.
- Visualize and analyze the 65 Turkish provinces (initially described by the 8 variables) on a lower dimensional map, the optimal view for the variability criterion.
- Build a set of few uncorrelated PCs representing a large proportion of the dataset total variability.

## 2.7 Hierarchical Agglomerative Cluster (HAC) analysis

Once computed the few PCs that allow us to describe the most of the variability of the dataset in a low dimensional space, we grouped the units by means of a hierarchical agglomerative clustering (HAC) analysis on the cloud of observations projected onto this new space. We applied the Ward's agglomerative method (which uses a of variance criterion, like the PCA) with the standard Euclidean distance. Applying the HAC to the data projected onto the principal factorial axes of the PCA contributes to improve the clustering robustness, since it retains the most important dimensions regarding the structure of data, without incorporating dimensions usually associated with “noise” or observation errors.

The optimal number of clusters was estimated as the most voted by the four different tests available in Matlab (Calinski-Harabasz (Caliński & Harabasz, 1974), Davies-Bouldin (Davies & Bouldin, 1979), Gap index (Tibshirani, Walther, & Hastie, 2001) and Silhouette index (Rousseeuw, 1987)), and assuming an initial range between 2 and 10 clusters.

## 3 Results

### 3.1 Principal Component Analysis (PCA)

#### *Eigenvalues and explained variance*

The first column of Tab. 3 contains the eigenvalues, which reflect the quality of the reduction from the 8-dimensional initial dataset to a lower number of dimensions. These eigenvalues (variances) are relatively small which was somehow expected, since the PCA was applied to the correlation matrix generated by the original data set (instead of the covariance matrix). In our case, we can see that the first eigenvalue equals 2.41 and represents 30% of the total variability, while the second one equals 2.11 and represents 26% of the total variability (second column of Tab. 3). This means that if we project the data on the space defined only by the first two principal components (PC1 and PC2), we will still be able to observe 56% of the total variability of the data (column 3 of Tab. 3).

The last two columns of Tab. 3 are visualized in the Scree Plot (Fig. 16). This is a graphical representation of the percentages of the variation that each PC accounts for. Now we need to decide what is the optimal number of dimensions that allows us to reduce the dimensionality of the dataset and, at the same time, describe its variability in the best way possible.

To decide the optimal number of dimensions to retain we employed two commonly found criteria:

- The components should explain a minimum of 80% of the total variance (which is equal to the number of variables).
- Each eigenvalue is greater than the average value one (Kaiser rule).

In view of these two rules we decide to reduce the dimensionality of the data set from 8 to 4 variables (being more conservative with respect to the Kaiser rule, since the eigenvalue is only slightly inferior to one).

	Eigenvalue	Variance (%)	Cumulative Variance (%)
<b>PC1</b>	2.41	30	30
<b>PC2</b>	2.11	26	56
<b>PC3</b>	1.27	16	72
<b>PC4</b>	0.998	12	85
<b>PC5</b>	0.56	7	92
<b>PC6</b>	0.40	5	97
<b>PC7</b>	0.18	2	99
<b>PC8</b>	0.08	1	100

Tab. 3. Each eigenvalue corresponds to a PC variance, and each PC to a linear combination of the initial (standardized) variables, and all the PCs are uncorrelated. The eigenvalues and the corresponding PCs are sorted by decreasing order their explained variance. The last column represents the cumulative percentage of explained variance.

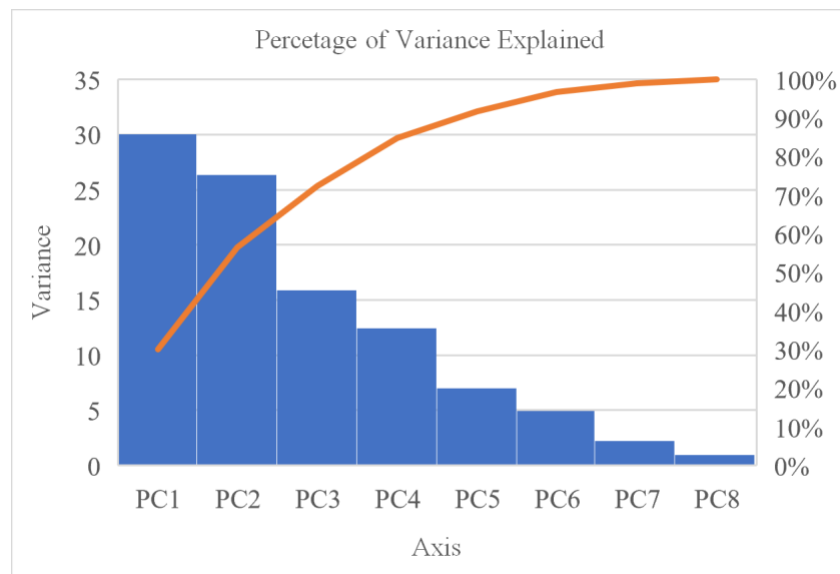


Fig. 16. Graphical representation of the percentages of variance that each PC accounts for together with the scree plot of the cumulative percentage of explained variance.

### *Coefficients and correlation table*

The PCs are created to maximize the amount of variance whilst remaining uncorrelated with each other, so there is not necessarily a simple interpretation of their structure.

Tab. 4 shows the coefficients (loadings) of the principal components as linear combinations of the original standardized variables, with the variables that are more correlated with the principal

components written in bold. Absolute values near zero indicate that a variable contributes very little to the component, whereas larger absolute values indicate the opposite.

The square of the coefficients presented in Tab. 4 give the relative importance of each variable to the construction of each component, but in order to obtain the correlation coefficients between variables and principal components, we need to multiply the values of Tab. 4 by the square roots of the PC eigenvalues, as displayed in the Tab. 5. Focusing on this table, we can see that the first component (PC1) essentially captures *spatial* aspects of the fire regime: fire incidence, as represented by the number of active fires (ICAF) and total area burned (ICAB). The second component (PC2) captures the *temporal* dimension: season length (SL) and modality (MT). The largest correlation coefficient for the third component (PC3) is interannual variability of recorded area burned (CVAB) and for the fourth one (PC4) is the percentage of years when the fire peak month is a summer month (PSPM).

Therefore, while the first PC capture spatial behavior of fire regimes, the other three are descriptors of the temporal dimension.

Var/PCs	PC1	PC2	PC3	PC4	PC5	PC6	PC7	PC8
<b>ICAF</b>	<b>0.56</b>	0.24	0.07	-0.25	-0.08	0.19	-0.17	-0.70
<b>CVAF</b>	0.01	-0.43	0.40	-0.50	-0.09	-0.63	-0.03	-0.08
<b>ICAB</b>	<b>0.56</b>	0.17	0.09	-0.34	0.00	0.13	-0.13	0.70
<b>CVAB</b>	-0.32	-0.18	<b>0.61</b>	-0.18	-0.14	0.67	-0.02	0.01
<b>SL</b>	-0.07	<b>0.59</b>	0.34	-0.07	0.00	-0.17	0.71	-0.01
<b>MT</b>	0.24	<b>-0.51</b>	-0.36	-0.20	0.00	0.26	0.66	-0.04
<b>PSPM</b>	0.34	-0.17	0.25	<b>0.58</b>	-0.67	-0.09	0.09	0.05
<b>IT</b>	0.31	-0.22	0.40	0.41	0.72	-0.02	0.06	-0.04

Tab. 4. Coefficients (loadings) table

Var/PCs	PC1	PC2	PC3	PC4	PC5	PC6	PC7	PC8
<b>ICAF</b>	<b>0.86</b>	0.35	0.07	-0.25	-0.06	0.12	-0.07	-0.20
<b>CVAF</b>	0.01	-0.62	0.45	-0.50	-0.07	-0.40	-0.01	-0.02
<b>ICAB</b>	<b>0.87</b>	0.25	0.10	-0.34	0.00	0.08	-0.06	0.20
<b>CVAB</b>	-0.49	-0.27	<b>0.68</b>	-0.18	-0.11	0.42	-0.01	0.00
<b>SL</b>	-0.10	<b>0.86</b>	0.38	-0.07	0.00	-0.11	0.30	0.00
<b>MT</b>	0.37	<b>-0.75</b>	-0.40	-0.20	0.00	0.17	0.28	-0.01
<b>PSPM</b>	0.53	-0.24	0.28	<b>0.58</b>	-0.50	-0.06	0.04	0.01
<b>IT</b>	0.48	-0.33	0.45	0.41	0.54	-0.01	0.03	-0.01

Tab. 5. Correlations between variables and factors

### *Correlation spheres*

When more than two PCs are selected to describe the variability of the dataset, a good way to display the correlation patterns between variables and interpreting the meaning of the new factorial dimensions is through the *correlation spheres* (Fig. 17). Since we selected four PCs and we can only represent maximum three dimensions at a time, we decide to represent the relationships between the variables in the new factorial space in the most meaningful way possible by plotting the correlation spheres of the first three PCs (accounting for 72% of the variance) and the first two PCs and the fourth one (accounting for 68% of the variance).

The coordinate axes are the selected PCs, while the vectors represent the variables, with coordinates given by the correlations between the variable and the three PCs. Vector length shows how well a variable is represented in the three PCs dimensions. A vector length close to one means that the variable is well represented in the space defined by the three PCs. If, in addition, one has a small angle between the vector and the dimension, the vector is represented in red, meaning that that dimension can be associated with the information carried out by the variable. For instance, in the correlation sphere of the first three PCs (Fig. 17a), the first PC can be associated with fire incidence (ICAF and ICAB), the second PC with the temporal distribution of the active fires, respectively, and opposite to each other, Season Length (SL) and Modality (MT), while the third dimension can be associated, in a lesser strong way, with the interannual variability of the detected burned area (CVAB).

On the other hand, if a variable has a small vector length, the variable is better represented on other PC dimensions and the vector is represented in black. For instance, the variable representing the seasonality of the fire activity (PSPM), does not give a relevant contribution in any of the first three PCs but is well represented on the fourth PC (Fig. 17b), that we can consider a fire seasonality dimension.

The angle between the vectors gives an approximation of the correlation between the respective variables when the variables are well represented in the correlation sphere. A small angle indicates the variables are positively correlated. For instance, considering the correlation sphere associated with PC1-PC2-PC4 axes, we can see that the variable summer activity (PSPM) and intensity (IT) are positively correlated, as we can be expected in Turkey. An angle close to 90 degrees indicates the variables are uncorrelated. In our case, we can say that fire incidence is not correlated with season length nor with its modality. An angle close to 180 degrees indicates that the variables are

inversely correlated. For instance, the length of the fire season (SL) is inversely correlated with the percentage of unimodal years (MT). In fact, a long season is more likely to have a multimodal behavior. The values of the correlations between the variables are reported in the Appendix D.

To summarize we can say that:

1. PC1 opposes provinces with high fire incidence versus those with low activity
2. PC2 opposes provinces with long fire seasons and lower percentage of unimodal seasons versus those with short fire seasons and higher percentage of unimodal seasons,
3. PC3 separates provinces with high interannual variability of recorded burned area from those with lower variability.
4. And to a lesser extent, PC4 separates provinces with predominant summer activity and more intense fires from provinces with fire activity occurring outside the summer months.

These trends will be helpful in interpreting the next plots. From now on, we will refer to the new dimensions with the abbreviation of the variables better represented on them. So respectively:

- PC1 → ICAF, ICAB
- PC2 → SL, -MT. The negative sign represents the inverse relationship with the other unsigned variable
- PC3 → CVAB
- PC4 → PSPM

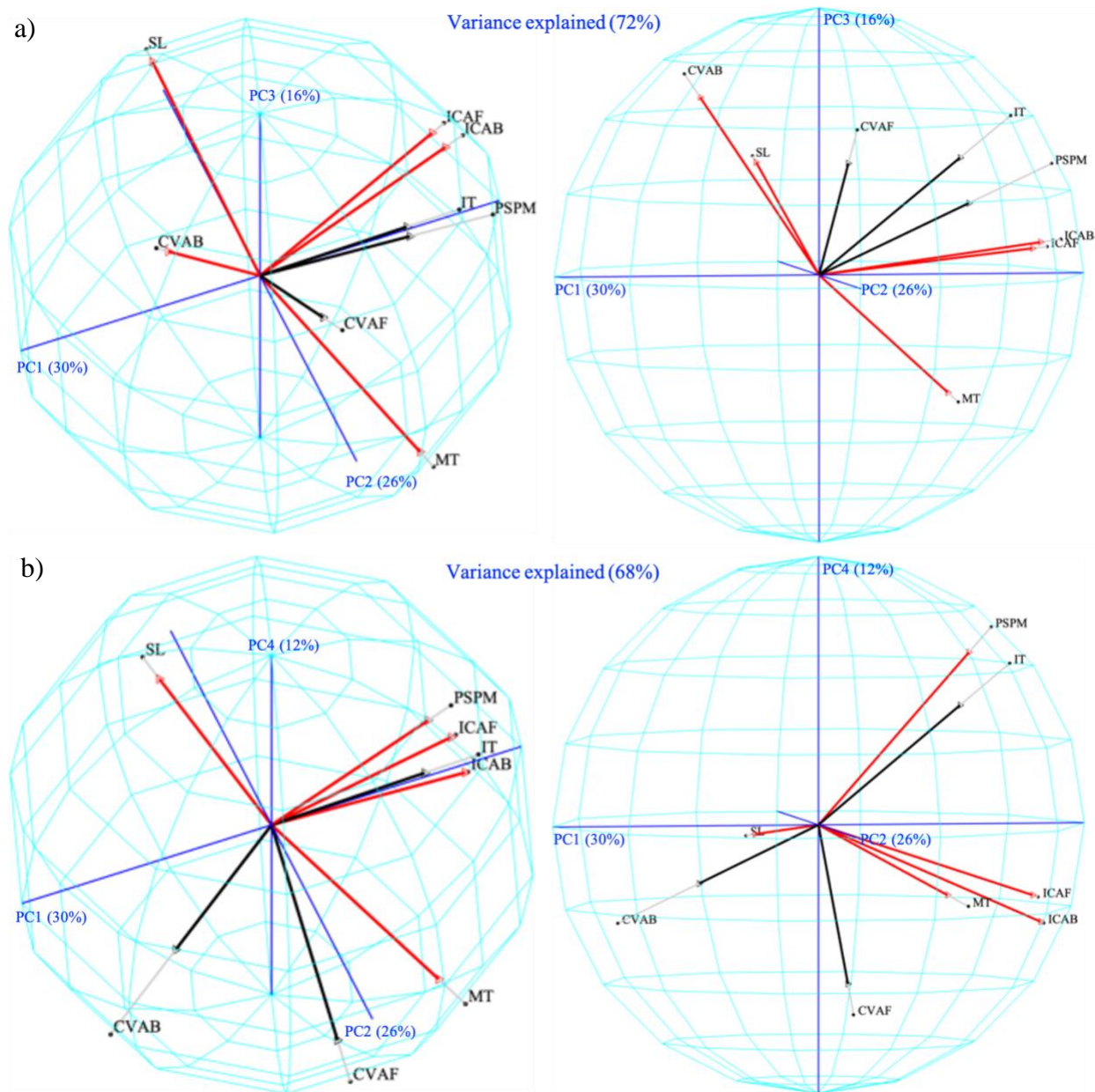


Fig. 17. Correlation spheres.

### 3.2. Clusters and classification of fire regimes

#### *Grouping the units into clusters of similar characteristics*

The hierarchical agglomerative clustering analysis was performed on the cloud of observations projected onto the selected four principal components described above. The HAC allows to group units with similar characteristics in a hierarchical structure represented by a tree called dendrogram (Fig. 18). The dendrogram y-axis can be used to evaluate the similarity between clusters. In order

to obtain the final segmentation, the dendrogram can be cut at a level that generates the desired number of groups.

We clearly see three cluster profiles in the dendrogram. This number is confirmed by the two classical metrics for evaluating clustering processes: Calinski-Harabasz, and Davies-Bouldin. While Gap and Silhouette indexes suggest ten and two clusters respectively.

The sequence of dendrogram splits first identifies a small cluster of only five units (in blue), while the following split recognizes other two clusters that include all the remaining provinces, almost equally distributed between them. From left to right, the first one, in red, has 27 units, and the second one, in green, 32 units. Inside each one the first two large clusters, a further split would identify two groups, with a smaller cluster of 10 units (pink) in the first largest cluster, and two more groups, with a smaller group of 7 units (dark-green) in the second one.

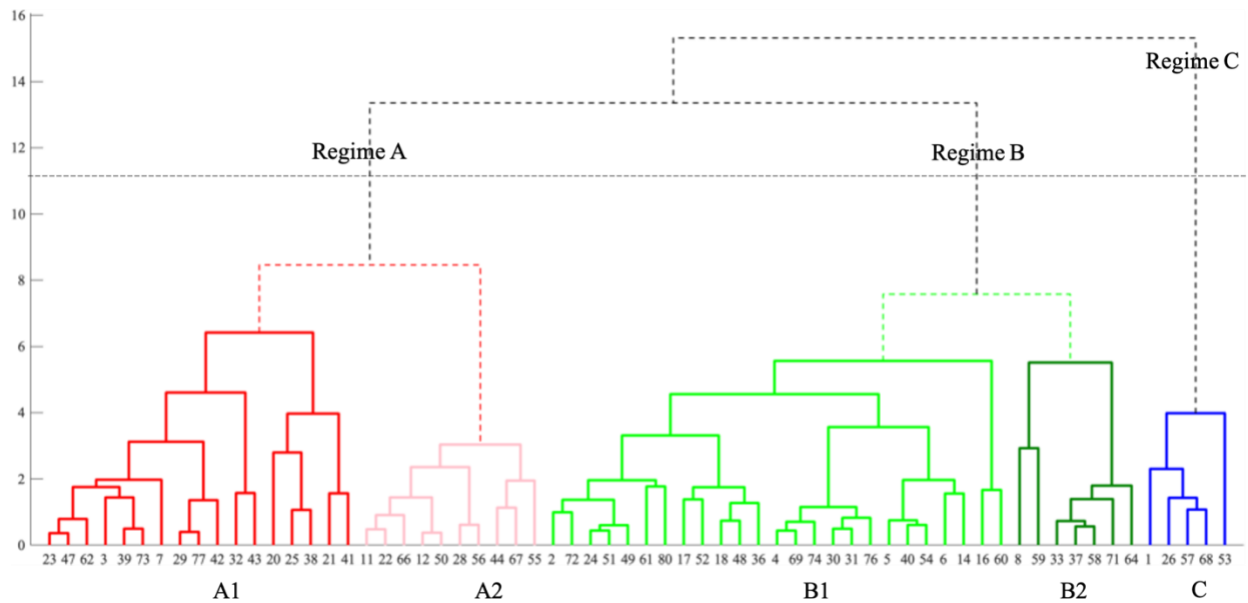


*Fig. 18. Dendrogram produced by the hierarchical clustering method applied to the first four PCs. The vertical axis represents the merging costs defined by Ward's method.*

### *Understanding the similarities between observations*

So far, we have explained the relationships between the variables and how they are represented in the space of the first four PCs (accounting for more than 80% of the variability in the dataset), and how the HAC allows us to define clusters of units with similar characteristics starting from observations projected onto these new dimensions.

In Fig. 19 the colors of the units and their convex envelopes represent the groups defined by the HAC. The shape and position of the convex hulls provide visual information on the observations (units) of each cluster, regarding the variables more correlated with the four principal axes.

Additionally, the distribution of the values of the eight quantitative variables in the clusters is displayed by means of the box-plots in Fig. 20. Taking into account the information on the central tendency (i.e., median) and dispersion of the values in the clusters together with the above information on the factorial space, for the variables better represented in the reduced factorial space, fire incidence, inter-annual variability, seasonality and intensity, we produced a synthetic description of the clusters in terms of *sensu stricto*. A more detailed account on this classification is done in discussion section.

The first fire regime identified by the sequence of dendrogram splits (in blue), **Regime C** is characterized by high incidence, regular activity and medium-long season. The other two fire regimes identified by the next split in the dendrogram have been renamed Regime A and Regime B.

**Regime A** (in red/pink) is characterized by low incidence and regular activity, with long (often bimodal) fire season, with small winter activity for the Sub-Regime A1 (in red), and short unimodal season with relevant winter activity for the Sub-Regime A2 (in pink).

**Regime B** (in light/dark green), is characterized by medium-low incidence, short unimodal season, with high interannual variability and small winter activity for the Sub-Regime B1 (in light green), and regular, intense and almost exclusively summer activity in the case of Sub-Regime B2 (in dark green).

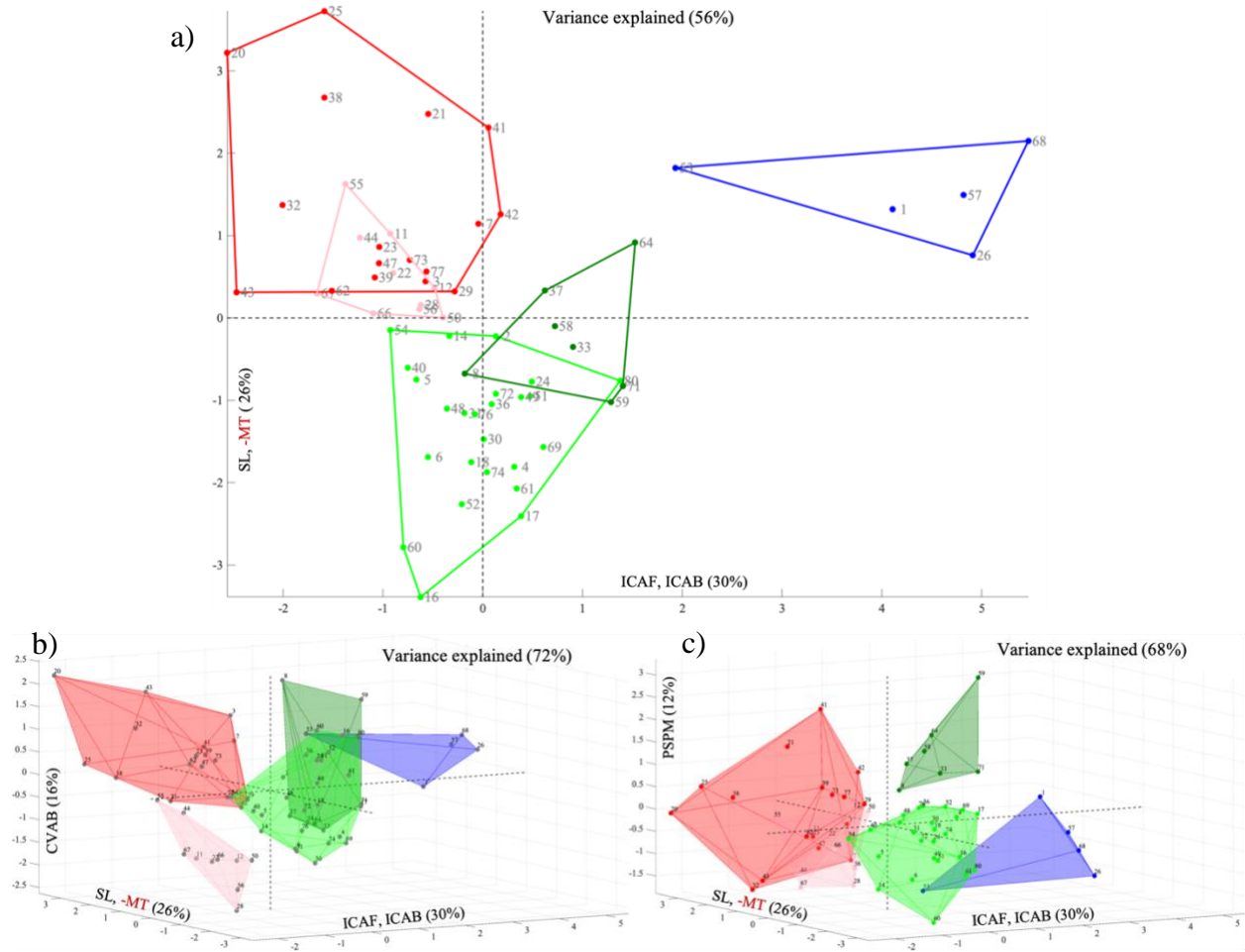


Fig. 19. Scatter plots of the observations within their convex envelopes, colored according to the clusters they belong to. These observations are projected on the factorial space, defined by: (a) the first two PCs, (b) the first three PCs, (c) the first two and the fourth PC.

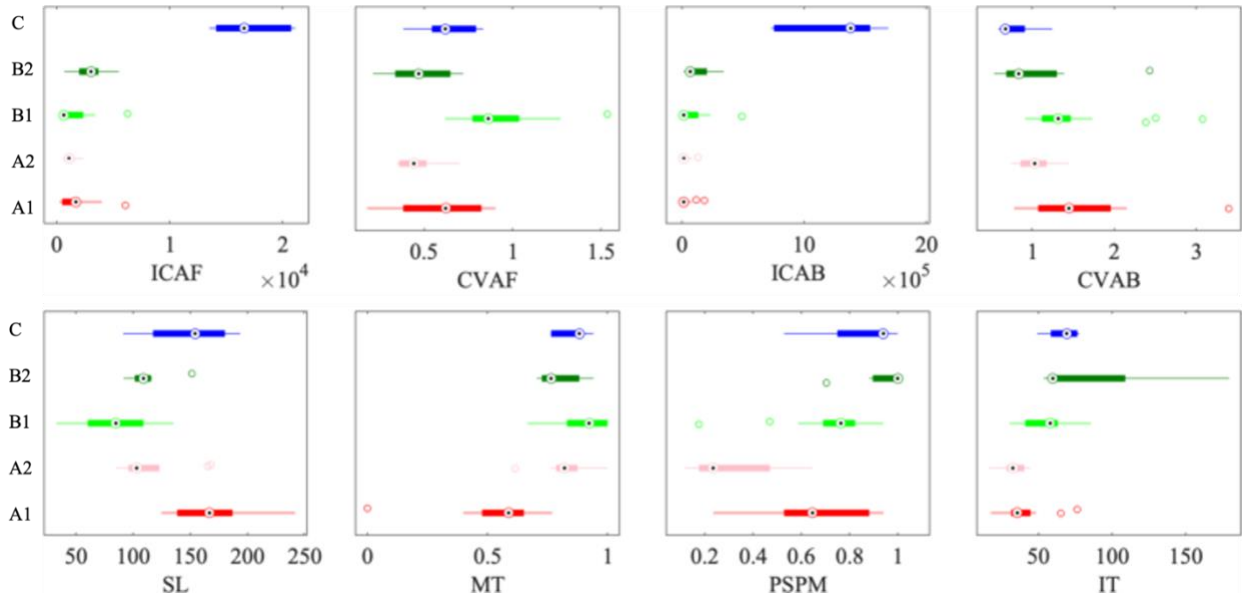


Fig. 20. Value distributions of fire regime variables. The black dot indicates the median, whereas the left and right edges of the colored box indicate the 25th and 75th percentiles, respectively. The colored circles indicate outliers.

Fig. 21 maps the distribution of the three identified fire regimes. Regime A prevails in North West Turkey, with a consistent group of provinces also located in the South East of Central Anatolia. Regime B is predominant in North East of Central Anatolia, in East and South Anatolia, while Regime C is mainly located in S-E Anatolia, except for one unit in the East of the Mediterranean region and one large province in Central Anatolia.

Despite being the smallest in terms of geographical extension (only 15% of the study area), the group of provinces belonging to fire Regime C, is the most relevant in terms of fire activity, accounting for almost 50% of the active fires (AF) and more than 60% of the area burned (AB) recorded from 2003 to 2019 (see Fig. 22). Follows fire Regime B (30% of AF and AB) and A (22.6% of AF and 9.5% of AB).

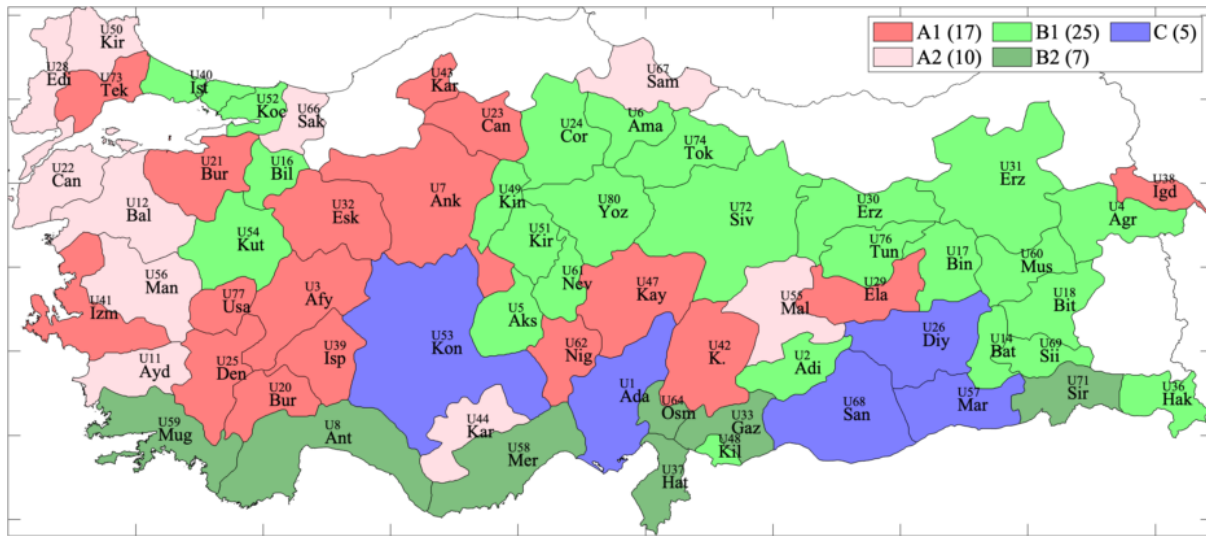


Fig. 21 low incidence, medium-long (often multi-unimodal) seasons, medium (A1) low (A2) interannual variability of recorded burned area; B: medium incidence, medium-short (unimodal) seasons, with more intense, highly variable and predominantly summer activity

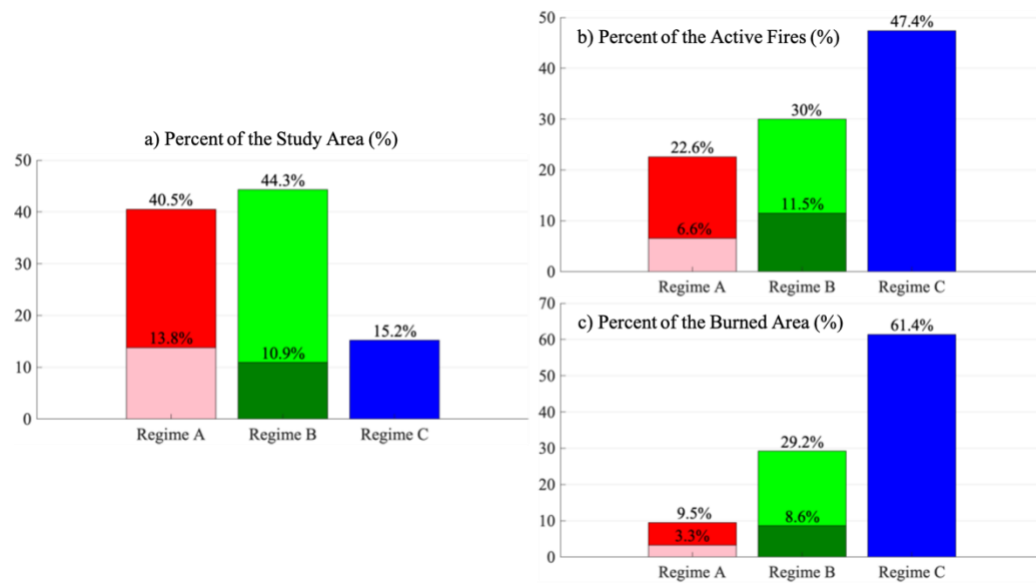


Fig. 22. Percentage of total area (a), number of active fire (b) and total area burned (c) that belongs to each of the three fire regimes.

### 3.3. Sensu lato fire regime characterization: anthromes and climate types

After interpreting the outputs of the PCA and HAC with the *sensu stricto* fire variables, we tried to let these outputs be even more informative by using the *sensu lato* qualitative variables *anthromes* and *climate types*. In this case, the *sensu lato* variables are called supplementary variables, and in fact, they are not taken into account in the PCA computation, but they are only

used to interpret the outputs, once computations are done. Each modality of a supplementary categorical variable is projected, in each factorial dimension, in the centroid of the units having that modality.

Fig. 23a shows the centroids associated with the *sensu lato* variables in the scatter plot of the observations projected onto the factorial space defined by the first two PCs helping us to understand the links between the *sensu stricto* variables well represented by these two components and the *sensu lato* variables. This kind of figure, together with a visual analysis of the identified regimes on the Anthromes and Climate type maps, helps us to derive further information about of them, in terms of antecedent characteristics.

**Regime A** is found mainly in (A1) *croplands-forests/villages* in transition from cold to temperate climate and (A2) *croplands-forests* in *temperate, dry summer* climate (Köppen type Cs).

**Regime B** occurs mainly (B1) in *croplands/rangelands-villages* in *cold, dry summer* climate (Ds), and (B2) in *forests* in *temperate, dry summer* climate (Cs).

**Regime C** is typical of the *residential irrigated croplands* of Southeastern and Central Anatolia and Southeastern Mediterranean Turkey with *temperate, dry summer* climate (Cs).

Anthrome centroids help us to understand the separation of the clusters along the new dimensions. Moving along PC1 (the incidence dimension) we go from higher to lower values as we go from *croplands* (Cr) to *forests* (Fo) for the aggregated classes and from *residential irrigated* (RI) to *populated rainfed* (PR) and *remote* (Rm) for the cropland classes. This can be explained with the fact that burning in croplands is intentionally used as agricultural practice, while forest fires receive much more pressure to be avoided or promptly suppressed once detected. Furthermore, high percentage of rural population and availability of water are linked with more intense agricultural activity and, as consequence to higher burning activity where fires are used periodically as land management tool.

On the second PC (the time dimension), we can notice how population density and climate type have an impact on the duration and regularity of the fires. We observe longer, often bimodal and more regular seasons, as we move from the cold (Ds) and scarcely populated *rangelands* and *villages* of the East to the temperate (Cs) more populated *croplands* and *villages* of the West.

Fig. 23b-c offer a 3D visualization of the convex hulls defining the clusters, allowing to visualize the contribution of the *Sensu Lato* centroids in separating the regimes along the variable CVAB (better represented on PC3) and PSPM (better represented on the PC4). There is very small

difference in the relative positions of the centroids along the third PC, such to further describe the fire regimes in terms of antecedent variables along these dimensions. While, along the fourth PC, we can notice that fire activity outside the summer period is more likely to happen in *croplands* rather than in *forests* and, within *croplands*, it is more likely to happen in *populated rainfed croplands* and *remote croplands* rather than in *residential irrigated croplands*. This can be explained with the fact that burning outside the summer period is more likely to occur where it is intentionally lid for agricultural practices.

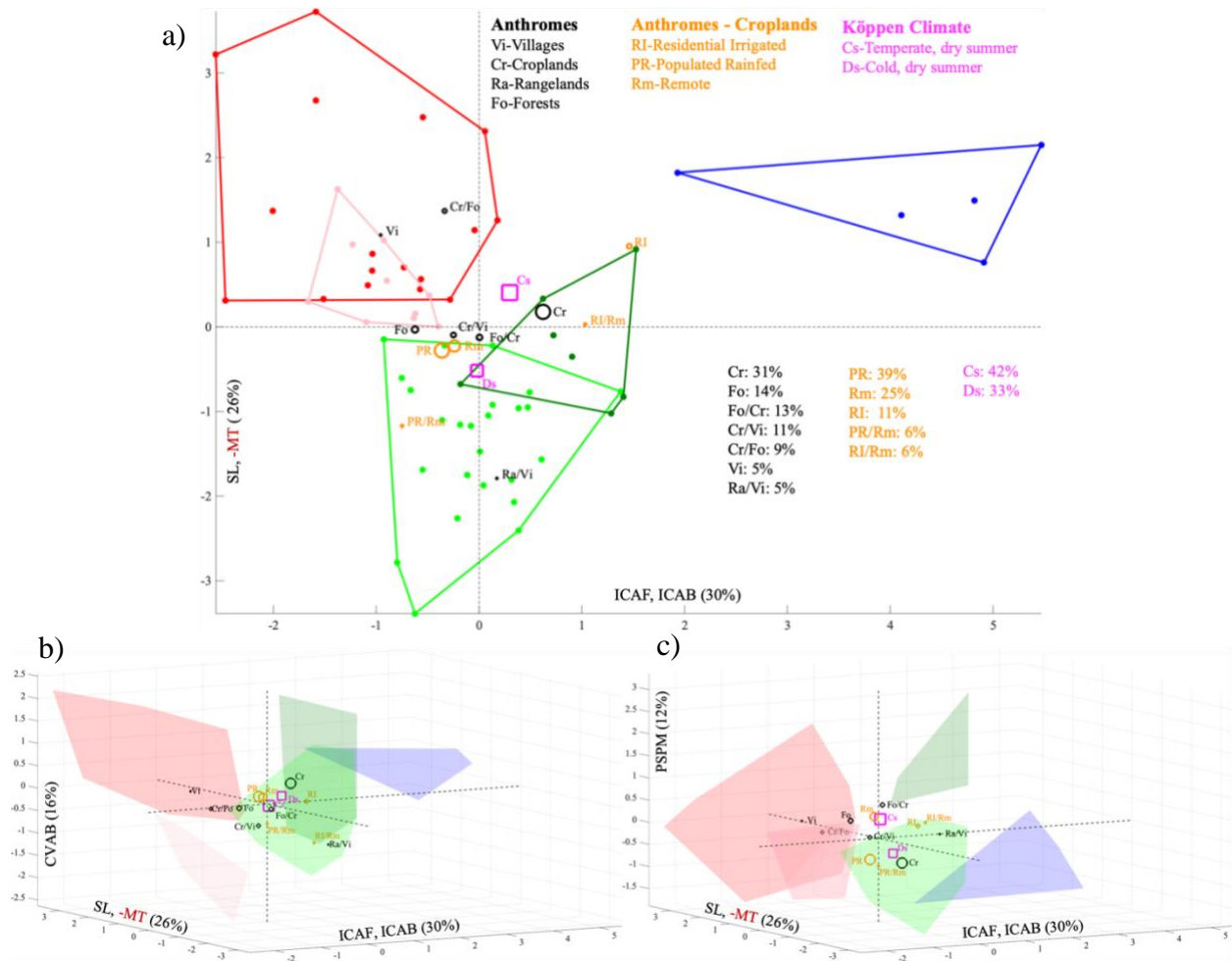


Fig. 23. Scatter plots of the observations within their convex envelopes, colored according to the clusters they belong to, projected in the space of: (a) the first two PCs, (b) the first three PC, (c) the first two and the fourth PC. The modalities of the antecedent variables are projected in the centroids of the units having these modalities and identified by black and orange circle respectively for Anthromes - aggregated classes and Anthromes - Croplands and by magenta squares for the Köppen climate types. The size of the dots representing the modalities of the antecedent variables is proportional to the percentage of the total number of units each modality represents.

The characteristics of the clusters with respect to the *sensu stricto* and *sensu lato* variables are summarized in Tab. 6. In the next session we will use this table as reference to unfold the pyrogeographical patterns identified and their main drivers.

Regimes	Sensu Lato			Sensu Stricto	
	Ant. Agg.	Ant. Crop.	Cli.		
<b>A: 27 units</b> <b>22.6% AF</b> <b>9.5% AB</b>	Cr, Fo	PR,Rm	Cs,Ds	Low incidence, regular, long season, often bimodal, sporadic winter activity, low intensity	short season, unimodal relevant winter activity
	Fo, Cr	PR, Rm	Cs		
<b>B: 32 units</b> <b>30% AF</b> <b>29.2% AB</b>	Cr, Vi	PR, Rm	Ds, Cs	Low incidence, irregular, short season, unimodal, sporadic winter activity, intense	regular
	Fo, Cr	Rm, RI	Cs		no winter activity
<b>C: 5 units</b> <b>47.4% AF</b> <b>61.4% AB</b>	Cr	RI	Cs	High incidence, regular long season, unimodal no winter activity, intense	

Tab. 6. Fire characteristics and classification of the fire regimes.

Anthromes - Aggregate: Vi: Villages; Cr: Croplands; Ra: Rangelands; Fo: Forests.

Anthromes - Croplands: RI: Residential Irrigated; PR: Populated Rainfed; Rm: Remote.

Climate types: Cs: Temperate, dry summer; Ds: Cold, dry summer.

## 4 Discussion

### 4.1 Fire regime characteristics and their main drivers

#### *Regime C: high incidence*

Large part of the variability in the dataset is determined by the fire incidence, the main responsible for separating the clusters along the first PC. Most of the fire activity observed by MODIS during the past 17 years, both in the form of active fires (47%), both in the form of burned area (60%), is concentrated in 15% of the study area, represented by the South Eastern provinces of Sanliurfa (U68), Mardin (U57) and Diyarbakir (U26), the close by Mediterranean province of Adana (U1) and in the large Central Anatolian province of Konya (U53).

This fire regime is characterized by agricultural burning of medium-high intensity, with larger fire season for the Mesopotamian provinces (4 to 6 months), with peak activity at the beginning of the summer, and for Konya (6.5 months), and a smaller fire season (3 months) for Adana with burnings concentrated more towards the end of the summer in the case of these last two provinces.

Such an intense fire activity coincide with vast agricultural areas identified as residential irrigated croplands. In Turkey, fires are ignited as common practice to burn croplands after the harvest.

These provinces are characterized by semi-arid to arid climate and cultivation during the dry summer months requires irrigation for successful crop development. The recent expansion of irrigated agriculture, coupled with high irrigation water requirements led to a 54% increase in agricultural water requirements between 1992 and 2017 (“AQUASTAT database ,” n.d.). “In the case of the South-East Anatolia Project, the expansion of irrigated cotton cultivation successfully boosted the regional economy, yet this occurred at the cost of drastic water consumption increases” (Rufin et al., 2019).

#### *Regimes A and B: low incidence*

Moving towards lower values of fire incidence we find the other two fire regimes, A and B. These two groups are much larger and together represent 85% of the study area but only 53% and 40% of recorded active fires and burned area respectively.

They are separated along the second PC mainly by the temporal behavior of the fire regimes.

*Sub-regime B1: short, irregular seasons*

The cold highlands of Central and East Anatolia are characterized by a more irregular fire season, quite short (two months) in the rangeland/cropland-village dominated provinces of East Anatolia and longer (up to four months) in the croplands of the Central Anatolia. Burning is concentrated in the summer season and show unimodal behavior with peak activity towards the end of the summer. The relatively high fire intensity recorded in many provinces with this fire regime can be related to grassland fires. In this case, larger available fuel loads tend to have greater combustion completeness and release a greater proportion of their total theoretical heat yield (Roberts et al., 2005).

*Sub-regime A1: long, bimodal seasons*

On the opposite side of the second PC there are the cropland and forest dominated provinces of Western Turkey, in transition from cold to temperate climate, and the cropland and village one of Southern Central Anatolia cold climate.

As we move towards the West and South of the country we found higher population density. Here burning is more regular and the fire season is longer (between five and six months) and often with bi-modal behavior. The burning activity is of medium-low intensity and occurs mainly in the summer, with relevant non-summer activity recorded in a few provinces (Burdur (U20), Denizli (U25), Eskişehir (U32) and Kayseri (U47)).

*Sub-regime A2: regular seasons, winter activity*

As we move along the third PC, redefined as variability dimension, we can further discriminate a distinct group of provinces out of regime A. It is the most homogeneous group in terms of internal variance. It is characterized by burning with low interannual variability and intensity, distributed along unimodal short seasons with peak activity more often occurring outside the summer period, generally in October.

This fire activity is mainly located in the most western part of the Anatolia and Thrace, in temperate climate, with high population density, where cropland and forest are the dominant landcovers. The timing and the regularity of burning could be associated to farming practices specific of this part of Turkey. Further investigation is needed.

### *Sub-regime B2: energetic summer fires*

The fourth PC gives information about how much the fire activity is concentrated in the summer months, and is highly correlated with the intensity of burning. Looking at the factorial space built with this dimension (Fig. 19c), we can notice that the sub-regime B2, separates well from its main cluster towards higher values of summer activity and fire intensity. This group of provinces located all along the south coast of Turkey from Muğla to Hatay, plus the South Est province of Sirnak (U71), is characterized by regular burning, distributed with unimodal short season with peak activity almost always occurring during the summer. The fire activity is intense and similar to the other two energetic fire regimes (C and B1), a part for the most Western provinces of Antalya (U8) and Muğla (U59) where the values of the recorded fire radiative power are respectively double and triple of the average of the group.

Long-lasting periods with hot and dry weather in summer, combined with warm and rainy winters, typical of Mediterranean climate, favor the accumulation of biomass before the summer and the condition for large energetic outbreaks during the summer.

In recent years, in these forest and remote cropland dominated provinces, climatic changes and socio-economic factors have increased the risk of burning of large areas (Ertuğrul & Varol, 2016). The larger fire ever recorded in the history of modern Turkey occurred at the beginning of August 2008 in the province of Antalya. It burned for 5 consecutive days and affected 15 795 ha of forestland mainly dominated by Turkish red pine (*Pinus brutia* Ten.), a typical fire adapted species of eastern Mediterranean basin ecosystems (Ürker, Tavşanoğlu, & Gürkan, n.d.). The fire was facilitated by extreme weather, which indicates that, even for a landscape that has not undergone yet a significant process of increasing fire hazard, as occurred in other Mediterranean countries, large fires can occur given suitable conditions (Viedma et al., 2017).

## 5 Conclusions

This study is the first aimed to produce a characterization of biomass burning over the entire land surface of Turkey. So far, all the available research on biomass burning in the country have been focused on the forested areas of Western Anatolia while a comprehensive study is still missing.

We used the most recent version of both the MODIS active fire (MCD14ML) and burned area (MCD64A1) products, to calculate eight fire regime variables to describe spatial, temporal and intensity behavior of fire regimes in 65 of the 81 Turkish provinces with relevant fire activity observed by MODIS during the past 17 years (2003-2019). We further characterized each province in terms of human produced ecological patterns and climate types by means of the most recent high resolution maps.

The PCA showed that much the of variability in the fire regime behavior across the Turkish provinces can be represented in a reduced four-dimensional space where incidence, temporality, interannual variability and seasonality are the most discriminant characteristics respectively.

The HCA on the dataset reprojected in this reduced space identifies an ideal number of three clusters, while two more sub-clusters have been considered form a visual analysis in order to interpret resulting geographical patterns.

Anthromes and climate types provided critical information in explaining the separation of the clusters along the new dimensions. High percentage of rural population and irrigation availability can be linked to the very high incidence observed in a cluster of only five provinces accounting for half of the MODIS recorded fire activity in the whole country. The cold and scarcely populated croplands and rangelands of Central and East Anatolia are characterized by short and mainly summer fire season with energetic occurrences, whereas the temperate and more populated croplands and villages of West and South-Center Anatolia present more regular and longer fire season, also outside the summer period with low energetic activity.

High intensity fires are associated with forests and remote croplands along the Mediterranean coast where climate change is increasing the risk of large outbreaks despite Turkish landscape has not undergone yet a significant process of increasing fire hazard as for the countries in the North West of the Mediterranean basin.

Further research, focus only on investigating the links between the identified fire regimes and the socio-economic dynamics and land management practice of the country is important in

order to embed the characterization of the fire regimes in a more comprehensive analysis of the complex interaction between anthropogenic and environmental drivers.

Increasing the number of variables and integrating additional meaningful datasets in their computation, as technology and algorithms are continuously improving, can help to advance the identification of the pyrogeographical patterns. A reduction of the spatial resolution of the analysis at the municipality level could also represent a further step in this direction.

## References

- Andela, N., Morton, D. C., Giglio, L., Paugam, R., Chen, Y., Hantson, S., ... Anderson, J. T. (2019). The Global Fire Atlas of individual fire size, duration, speed and direction. *Earth System Science Data*, *11*(2), 529–552. <https://doi.org/10.5194/essd-11-529-2019>
- Anderson, H. E. (1982). *Aids to Determining Fuel Models For Estimating Fire Behavior* THE AUTHOR.
- Andreae, M. O. (1993). The Influence of Tropical Biomass Burning on Climate and the Atmospheric Environment. In *Biogeochemistry of Global Change* (pp. 113–150). Springer US. [https://doi.org/10.1007/978-1-4615-2812-8\\_7](https://doi.org/10.1007/978-1-4615-2812-8_7)
- AQUASTAT database . (n.d.). Retrieved November 24, 2020, from <http://www.fao.org/nr/water/aquastat/data/query/index.html>
- Arca B.1, Pellizzaro G.1, Duce P.1, Salis M.2, 3, Bacciu V.2, 3, Spano D.2, 3, Ager A.4, Finney M.A.5, S. E. (2012). Modelling Fire Behaviour and Risk, (April 2014), 292.
- Atalay, I. (1986). Vegetation formations of Turkey. *Travaux - Institut de Geographie de Reims*, *65–66*, 17–30. <https://doi.org/10.3406/tigr.1986.1183>
- Atalay, Ibrahim. (2016). A New Approach to the Land Capability Classification: Case Study of Turkey. *Procedia Environmental Sciences*, *32*, 264–274. <https://doi.org/10.1016/j.proenv.2016.03.031>
- Atalay, Ibrahim, Efe, R., & Öztürk, M. (2014). Ecology and Classification of Forests in Turkey. *Procedia - Social and Behavioral Sciences*, *120*, 788–805. <https://doi.org/10.1016/j.sbspro.2014.02.163>
- Atmiş, E., Özden, S., & Lise, W. (2007). Urbanization pressures on the natural forests in Turkey: An overview. *Urban Forestry and Urban Greening*, *6*(2), 83–92. <https://doi.org/10.1016/j.ufug.2007.01.002>
- Balaban, U., & Fu, A. S. (2014). Politics of urban development and wildfires in California and Turkey. *Environment and Planning A*, *46*(4), 820–836. <https://doi.org/10.1068/a46163>
- Barros, A. M. G., & Pereira, J. M. C. (2014). Wildfire Selectivity for Land Cover Type: Does Size Matter? *PLoS ONE*, *9*(1), e84760. <https://doi.org/10.1371/journal.pone.0084760>
- Bekar, I., & Tavşanoğlu, Ç. (2017). Modelling the drivers of natural fire activity: The bias created by cropland fires. *International Journal of Wildland Fire*, *26*(10), 845–851. <https://doi.org/10.1071/WF16183>

- Caliński, T., & Harabasz, J. (1974). A Dendrite Method For Cluster Analysis. *Communications in Statistics*, 3(1), 1–27. <https://doi.org/10.1080/03610927408827101>
- Chen, D., Pereira, J. M. C., Masiero, A., & Pirotti, F. (2017). Mapping fire regimes in China using MODIS active fire and burned area data. *Applied Geography*, 85, 14–26. <https://doi.org/10.1016/j.apgeog.2017.05.013>
- Chuvieco, E., Giglio, L., & Justice, C. (2008). Global characterization of fire activity: Toward defining fire regimes from Earth observation data. *Global Change Biology*, 14(7), 1488–1502. <https://doi.org/10.1111/j.1365-2486.2008.01585.x>
- Çolak, A. H., & Rotherham, I. D. (2006). A review of the forest vegetation of Turkey: Its status past and present and its future conservation. *Biology and Environment*, 106(3), 343–354. <https://doi.org/10.3318/BIOE.2006.106.3.343>
- Cox, N. J. (2016). DIPTEST: Stata module to compute dip statistic to test for unimodality. *Statistical Software Components*.
- Davies, D. L., & Bouldin, D. W. (1979). A Cluster Separation Measure. *IEEE Transactions on Pattern Analysis and Machine Intelligence*, PAMI-1(2), 224–227. <https://doi.org/10.1109/TPAMI.1979.4766909>
- Davis, P. H. (1970). *Flora of Turkey and the East Aegean Islands*. Vol. 3. Edinburgh: University Press.
- Dozier, J. (1981). A method for satellite identification of surface temperature fields of subpixel resolution. *Remote Sensing of Environment*. [https://doi.org/10.1016/0034-4257\(81\)90021-3](https://doi.org/10.1016/0034-4257(81)90021-3)
- Ellis, E. C., Beusen, A. H. W., & Goldewijk, K. K. (2020). Anthropogenic biomes: 10,000 BCE to 2015 CE. *Land*, 9(5), 129. <https://doi.org/10.3390/LAND9050129>
- Ellis, E. C., & Ramankutty, N. (2008). Putting people in the map: Anthropogenic biomes of the world. *Frontiers in Ecology and the Environment*. Ecological Society of America. <https://doi.org/10.1890/070062>
- Ertugrul, M., & Varol, T. (2015). The relationship between fire number and burned area in Antalya, Izmir and Muğla regions in Turkey. *Journal of Environmental Biology*, 36(2), 399–403.
- Ertuğrul, M., & Varol, T. (2016). The Analysis of Large Fire Incidence in Turkey. *International Journal for Research in Applied Sciences*, 1(June), 1–8.
- European Commission. (2018). *JRC Technical Report Forest Fires in Europe, Middle East and*

*North Africa 2018*. Retrieved from <https://ec.europa.eu/jrc/en/publication/forest-fires-europe-middle-east-and-north-africa-2018>

European Forest Fire Information System (EFFIS). (2017). European Fuel Map, 2017, based on JRC Contract Number 384347 on the “Development of a European Fuel Map.” Retrieved August 17, 2020, from <https://effis.jrc.ec.europa.eu/about-effis/technical-background/fuels/>

Giglio, L., Boschetti, L., Roy, D., Hoffmann, A. A., & Humber, M. (2016). *Collection 6 MODIS Burned Area Product User's Guide Version 1.0 Abbreviations and Acronyms BA Burned Area CMG Climate Modeling Grid EOS Earth Observing System EOSDIS EOS Data Information System GeoTIFF Georeferenced Tagged Image File Format HDF Hierarchical Data Format LP-DAAC Land Processes Distributed Active Archive Center MODIS Moderate Resolution Imaging Spectrometer SDS Science Data Set QA Quality Assessment Title page image: MCD64A1 cumulative area burned in the Central*.

Giglio, L., Csiszar, I., & Justice, C. O. (2006). Global distribution and seasonality of active fires as observed with the Terra and Aqua Moderate Resolution Imaging Spectroradiometer (MODIS) sensors. *Journal of Geophysical Research: Biogeosciences*, 111(2). <https://doi.org/10.1029/2005JG000142>

Giglio, L., Descloitres, J., Justice, C. O., & Kaufman, Y. J. (n.d.). An Enhanced Contextual Fire Detection Algorithm for MODIS. [https://doi.org/10.1016/S0034-4257\(03\)00184-6](https://doi.org/10.1016/S0034-4257(03)00184-6)

Giglio, L., Schroeder, W., Hall, J. V., & Justice, C. O. (2018). *MODIS Collection 6 Active Fire Product User's Guide Revision B*.

Heward, H., Smith, A. M. S., Roy, D. P., Tinkham, W. T., Hoffman, C. M., Morgan, P., & Lannom, K. O. (2013). Is burn severity related to fire intensity? Observations from landscape scale remote sensing. *International Journal of Wildland Fire*, 22(7), 910–918. <https://doi.org/10.1071/WF12087>

Hijmans, R. J., Cameron, S. E., Parra, J. L., Jones, P. G., & Jarvis, A. (2005). Very high resolution interpolated climate surfaces for global land areas. *International Journal of Climatology*, 25(15), 1965–1978. <https://doi.org/10.1002/joc.1276>

JENKS, & F., G. (1967). The Data Model Concept in Statistical Mapping. *International Yearbook of Cartography*, 7, 186–190. Retrieved from <http://ci.nii.ac.jp/naid/10021899676/en/>

Kaiser, J. W., Boucher, O., Doutriaux-Boucher, M., Flemming, J., Govaerts, Y. M., Gulliver, J.,

- ... Wooster, M. J. (2009). Smoke in the air. *ECMWF Newsletter*, (119), 9–15.  
<https://doi.org/10.21957/ygoaoor6dm>
- Kottek, M., Grieser, J., Beck, C., Rudolf, B., & Rubel, F. (2006). World Map of the Köppen-Geiger climate classification updated, *15*(3), 259–263. <https://doi.org/10.1127/0941-2948/2006/0130>
- Krebs, P., Pezzatti, G. B., Mazzoleni, S., Talbot, L. M., & Conedera, M. (2010). Fire regime: History and definition of a key concept in disturbance ecology. *Theory in Biosciences*, *129*(1), 53–69. <https://doi.org/10.1007/s12064-010-0082-z>
- Lentile, L. B., Holden, Z. A., Smith, A. M. S., Falkowski, M. J., Hudak, A. T., Morgan, P., ... Benson, N. C. (2006, September 26). Remote sensing techniques to assess active fire characteristics and post-fire effects. *International Journal of Wildland Fire*. CSIRO PUBLISHING. <https://doi.org/10.1071/WF05097>
- MacArthur, R. H. (1957). ON THE RELATIVE ABUNDANCE OF BIRD SPECIES. *Proceedings of the National Academy of Sciences*, *43*(3), 293–295.  
<https://doi.org/10.1073/pnas.43.3.293>
- Martínez-Fernández, J., Chuvieco, E., & Koutsias, N. (2013). Modelling long-term fire occurrence factors in Spain by accounting for local variations with geographically weighted regression. *Natural Hazards and Earth System Sciences*, *13*(2), 311–327.  
<https://doi.org/10.5194/nhess-13-311-2013>
- Merlo, M., & Croitoru, L. (2005). *Valuing Mediterranean forests: Towards total economic value*. *Valuing Mediterranean Forests: Towards Total Economic Value*. CABI Publishing.  
<https://doi.org/10.1079/9780851999975.0000>
- Oliveira, S. L. J., Maier, S. W., Pereira, J. M. C., & Russell-Smith, J. (2015). Seasonal differences in fire activity and intensity in tropical savannas of northern Australia using satellite measurements of fire radiative power. *International Journal of Wildland Fire*, *24*(2), 249–260. <https://doi.org/10.1071/WF13201>
- Organisation for Economic Co-operation and Development (OECD). (2017). The Governance of Land Use - Country Fact Sheet Turkey, 5. <https://doi.org/10.1787/fae634b4-en>
- Özşahin, E., & Eroğlu, İ. (2020). (3) (PDF) *Spatiotemporal Change of Anthropogenic Biomes (Anthromes) of Turkey*. *Theory and Practice in Social Sciences*. Retrieved from [https://www.researchgate.net/publication/338384743\\_Spatiotemporal\\_Change\\_of\\_Anthrop](https://www.researchgate.net/publication/338384743_Spatiotemporal_Change_of_Anthrop)

ogenic\_Biomes\_Anthromes\_of\_Turkey

- Ozturk, M., Gucel, S., Kucuk, M., & Sakcali, S. (2010). Forest diversity, climate change and forest fires in the Mediterranean region of Turkey. *Journal of Environmental Biology*, 31(1–2), 1–9.
- Pereira, J., Sá, A., Sousa, A., Silva, J., Santos, T., & Carreiras, J. (1999). Spectral characterisation and discrimination of burnt areas (pp. 123–138).  
[https://doi.org/10.1007/978-3-642-60164-4\\_7](https://doi.org/10.1007/978-3-642-60164-4_7)
- Roberts, G., Wooster, M. J., Perry, G. L. W., Drake, N., Rebelo, L. M., & Dipotso, F. (2005). Retrieval of biomass combustion rates and totals from fire radiative power observations: Application to southern Africa using geostationary SEVIRI imagery. *Journal of Geophysical Research Atmospheres*. <https://doi.org/10.1029/2005JD006018>
- Rousseeuw, P. J. (1987). *Silhouettes: a graphical aid to the interpretation and validation of cluster analysis*. *Journal of Computational and Applied Mathematics* (Vol. 20).
- Roy, D. P., Boschetti, L., & Smith, A. M. (2013). Satellite Remote Sensing of Fires. In *Fire Phenomena and the Earth System: An Interdisciplinary Guide to Fire Science* (pp. 77–93). John Wiley and Sons. <https://doi.org/10.1002/9781118529539.ch5>
- Rufin, P., Frantz, D., Ernst, S., Rabe, A., Griffiths, P., Özdoğan, M., & Hostert, P. (2019). Mapping Cropping Practices on a National Scale Using Intra-Annual Landsat Time Series Binning. *Remote Sensing*, 11(3), 232. <https://doi.org/10.3390/rs11030232>
- Satir, O., Berberoglu, S., & Cilek, A. (2016). Modelling long term forest fire risk using fire weather index under climate change in Turkey. *Applied Ecology and Environmental Research*, 14(4), 537–551. [https://doi.org/10.15666/aecer/1404\\_537551](https://doi.org/10.15666/aecer/1404_537551)
- Sensoy Serhat, Demircan Mesut, U. Y. (2016). (5) (PDF) Climate of Turkey. Retrieved from [https://www.researchgate.net/publication/296597022\\_Climate\\_of\\_Turkey](https://www.researchgate.net/publication/296597022_Climate_of_Turkey)
- Tibshirani, R., Walther, G., & Hastie, T. (2001). Estimating the number of clusters in a data set via the gap statistic. *Journal of the Royal Statistical Society. Series B: Statistical Methodology*, 63(2), 411–423. <https://doi.org/10.1111/1467-9868.00293>
- Tolunay, A., & Türkoğlu, T. (1997). Effects of traditional goat farming on forest fire control in Turkey, 382–385.
- Turkish Statistic Institute. (2020). The Results of Address Based Population Registration System. Retrieved from <http://www.turkstat.gov.tr/PreHaberBultenleri.do?id=21507>

- Ürker, O., Tavşanoğlu, Ç., & Gürkan, B. (n.d.). Post-fire recovery of the plant community in *Pinus brutia* forests: active vs. indirect restoration techniques after salvage logging. <https://doi.org/10.3832/ifor2645-011>
- Ustaoglu, E., & Aydinoglu, A. C. (2019). Regional variations of land-use development and land-use/cover change dynamics: A case study of Turkey. *Remote Sensing*, *11*(7), 1–33. <https://doi.org/10.3390/RS11070885>
- Varol, T., Ertuğrul, M., & ÖZEL, H. B. (2018). The Analysis of the Forest Fires in Turkey with Statistical Quality Control Method. *Modern Management Forum*, *2*(1), 1–12. <https://doi.org/10.18686/mmfv2i1.975>
- Viedma, O., Moreno, J. M., Güngöroğlu, C., Cosgun, U., & Kavgacı, A. (2017). Recent land-use and land-cover changes and its driving factors in a fire-prone area of southwestern Turkey. *Journal of Environmental Management*, *197*, 719–731. <https://doi.org/10.1016/j.jenvman.2017.02.074>
- Wooster, M. J., Zhukov, B., & Oertel, D. (2003). Fire radiative energy for quantitative study of biomass burning: Derivation from the BIRD experimental satellite and comparison to MODIS fire products. *Remote Sensing of Environment*, *86*(1), 83–107. [https://doi.org/10.1016/S0034-4257\(03\)00070-1](https://doi.org/10.1016/S0034-4257(03)00070-1)
- Yılmaz, E., & Çiçek, İ. (n.d.). Türkiye İklim Araştırmaları - Coğrafya Bölümü. Retrieved August 11, 2020, from <http://geography.humanity.ankara.edu.tr/turkiye-iklim-arastirmalari/>
- Yılmaz, E., & Çiçek, İ. (2018). Detailed Köppen-Geiger climate regions of Turkey<p>Türkiye'nin detaylandırılmış Köppen-Geiger iklim bölgeleri. *Journal of Human Sciences*, *15*(1), 225–242. Retrieved from <https://www.j-humansciences.com/ojs/index.php/IJHS/article/view/5040>

# Appendices

## Appendix A: Turkish Province IDs and MODIS active fire counts

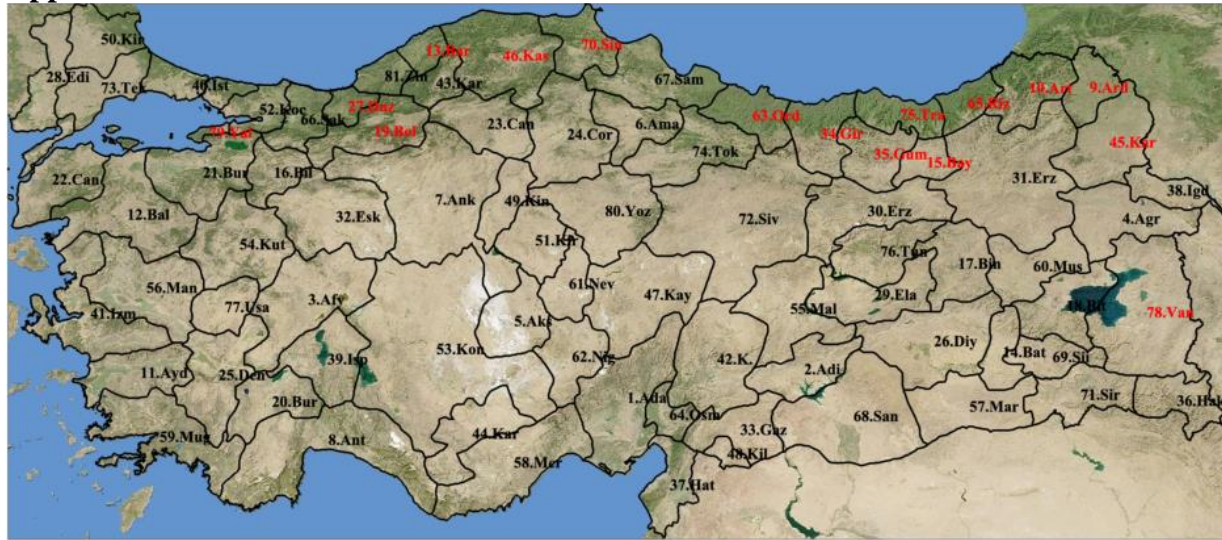


Fig.A 1. The 81 Turkish provinces with their respective identification number, assigned in alphabetic order. In red the provinces where the MODIS Active Fire Product (MCD14ML, collection 6) reported less than 170 active fires from March 2003 to December 2019. These provinces have been removed from the analysis.

ID	Province	MODIS Counts	ID	Province	MODIS Counts	ID	Province	MODIS Counts	ID	Province	MODIS Counts	ID	Province	MODIS Counts
68	Sanliurfa	21139	49	Kinkkale	2649	12	Balikesir	1140	43	Karabuk	430	75	Trabzon	101
1	Adana	20641	72	Sivas	2435	5	Aksaray	1043	62	Nigde	416	45	Kars	100
57	Mardin	16598	56	Manisa	2334	22	Canakkale	1039	17	Bingol	358	15	Bayburt	95
26	Diyarbakir	14319	28	Edirne	2321	6	Amasya	996	38	Igdir	358	70	Sinop	93
53	Konya	13503	14	Batman	2314	36	Hakkari	933	18	Bitlis	333	27	Duzce	77
80	Yozgat	6257	25	Denizli	2206	23	Cankiri	907	54	Kutahya	292	9	Ardahan	63
7	Ankara	6070	21	Bursa	2019	29	Elazig	800	31	Erzurum	290	79	Yalova	47
64	Osmaniye	5501	61	Nevsehir	1999	50	Kirklareli	714	4	Agri	244	63	Ordu	43
42	K. Maras	4004	47	Kayseri	1749	66	Sakarya	706	48	Kilis	238	35	Gumushane	42
37	Hatay	3781	3	Afyon	1727	59	Mugla	681	20	Burdur	236	34	Giresun	36
58	Mersin	3439	73	Tekirdag	1705	55	Malatya	649	76	Tunceli	236	13	Bartın	32
24	Corum	3417	32	Eskisehir	1701	60	Mus	629	52	Kocaeli	227	65	Rize	30
51	Kirsehir	3358	8	Antalya	1684	81	Zinguldak	597	30	Erzincan	220	10	Artvin	28
33	Gaziantep	3035	11	Aydin	1447	74	Tokat	560	16	Bilecik	194	<b>Total Counts (81 units)</b>		
71	Sirnak	2894	77	Usak	1403	67	Samsun	544	78	Van	148	<b>183820</b>		
41	Izmir	2879	44	Karaman	1197	39	Isparta	499	46	Kastamonu	135	<b>Total Counts (65 units)</b>		
2	Adiyaman	2743	69	Siirt	1178	40	Istanbul	478	19	Bolu	117	<b>182633</b>		

Tab.A 1. The 81 Turkish provinces with their respective identification number (ID), listed in decreasing order according to the number of MODIS active fires (MODIS Counts) from March 2003 to December 2019. In red the provinces where MODIS reported less than 170 counts. These provinces have been removed from the analysis.

ID	Province	ID	Province	ID	Province	ID	Province	ID	Province	ID	Province
1	Adana	16	Bilecik	29	Elazığ	42	K. Maras	55	Malatya	68	Sanliurfa
2	Adiyaman	17	Bingol	30	Erzincan	43	Karabuk	56	Manisa	69	Siirt
3	Afyon	18	Bitlis	31	Erzurum	44	Karaman	57	Mardin	71	Sirnak
4	Agri	20	Burdur	32	Eskisehir	47	Kayseri	58	Mersin	72	Sivas
5	Aksaray	21	Bursa	33	Gaziantep	48	Kilis	59	Mugla	73	Tekirdag
6	Amasya	22	Canakkale	36	Hakkari	49	Kinkkale	60	Mus	74	Tokat
7	Ankara	23	Cankiri	37	Hatay	50	Kirklareli	61	Nevsehir	76	Tunceli
8	Antalya	24	Corum	38	Igdir	51	Kirsehir	62	Nigde	77	Uzak
11	Aydin	25	Denizli	39	Isparta	52	Kocaeli	64	Osmaniye	80	Yozgat
12	Balikesir	26	Diyarbakir	40	Istanbul	53	Konya	66	Sakarya	81	Zinguldak
14	Batman	28	Edirne	41	Izmir	54	Kutahya	67	Samsun		

Tab.A 2. The selected Turkish provinces (65) with their respective identification number (ID), listed in alfabetic order.

## Appendix B: Season Length (SL) and Season Modality (SM) calculation

For each unit, first we defined which years were populated enough to be considered in the analysis. A fire occurrence at a given unit and day of year (DoY) was declared isolated if the number of fires in the interval  $[DoY-R, DoY+R] \leq K$ , with  $K=4$  (fires) and  $R = 90$ th percentile of the set of date differences between consecutive days with fire occurrences. The values of the parameters  $K$  and  $R$  were estimated empirically and provide a good combination for the definition of isolated fires. Only years that initially reported more than 20 fires occurrences and still kept at least 10 fire occurrences after the isolated fires removal procedure were selected for analysis.

For each unit and each one of the selected years, a kernel density curve was estimated based on the sample of the incidence values. The corresponding bandwidth was used to determine the location of the *modes* and *anti-modes*.

The overall fire season length (SL) is determined by the number of days between the DoY of the first and last *anti-modes*. In multimodal areas the season length reflects the sum of the durations of the seasons (Fig. B 1).

To calculate the season modality (SM), we first defined what is a *True Mode* and a *True Anti-mode*. To accomplish this, for each unit and for each selected year we calculate the local maxima and minima values of the kernel density function. Then we declare a mode as a *true mode* if it the corresponding value is greater than 0.4 times the maximum value of the kernel density function and we declare an anti-mode as a *true anti-mode* if its height is smaller than 0.1 times the above maximum value.

For a fire season in a specific unit and in a specific selected year, to be declared *non-unimodal*, the following criteria were used:

1. the distance between the first and the last *true mode* was larger than 90 days
2. there was at least one *true anti-mode* between them (Fig. B 1).

Finally, we defined the SM variable for each unit as the percentage of years declared as unimodal with respect to the total number of selected years (for that specific unit).

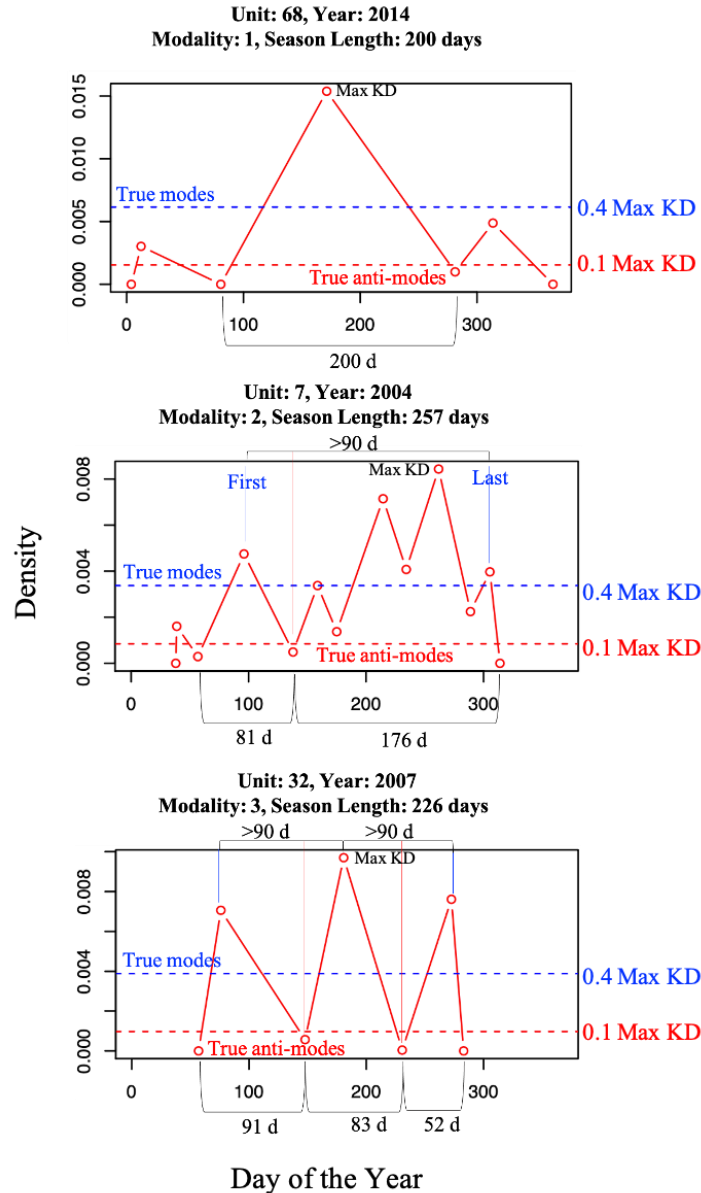


Fig. B 1. Polygonal lines defined by the true modes/anti-modes (right) for three units in three specific years, showing how the number of seasons and the season length is calculated. This is schematic representation of the kernel density function modes and anti-modes. KD: Kernel Density Function.

## Appendix C: Sensu Stricto and Sensu Lato variables

Unit	Name	<i>sensu stricto</i>								<i>sensu lato</i>		
		ICAF	CVAF	ICAB	CVAB	SL	MT	PSPM	IT	Ant. agg	Ant. Crop.	Cli.
		counts	[]	Km <sup>2</sup>	[]	days	[]	[]	MW px <sup>-1</sup>			
1	Adana	20641	0.38	760839	0.67	91	0.76	1.00	62	Cr/Fo	RI/Rm	Cs/Ds
2	Adiyaman	2743	0.79	132182	1.37	131	0.82	0.82	50	Cr	RI/PR	Cs
3	Afyon	1727	0.87	78157	1.78	175	0.65	0.71	65	Cr	PR	Cs/Ds
4	Agri	244	0.84	25327	0.96	65	1.00	0.81	61	Ra/Vi	PR	Df/Ds
5	Aksaray	1043	0.78	12636	1.52	106	0.92	0.59	38	Cr	PR	Ds/B
6	Amasya	996	0.88	15196	1.38	55	1.00	0.47	40	Cr	PR/Rm	Cs/Ds
7	Ankara	6070	0.88	186074	1.45	191	0.71	0.59	44	Cr	PR	Ds
8	Antalya	1684	0.72	30803	2.43	151	0.76	0.71	120	Fo/Cr	Rm	Cs
11	Aydin	1447	0.36	19485	0.86	123	0.76	0.24	40	Fo/Cr	RI/Rm	Cs
12	Balikesir	1140	0.35	36993	0.89	100	0.82	0.47	43	Fo/Cr	Rm/PR	Cs
14	Batman	2314	0.87	222962	0.93	96	0.81	0.18	54	Cr/Vi	PR	Cs
16	Bilecik	194	1.04	1594	3.08	33	1.00	0.88	72	Fo/Cr	PR/Rm	Cs
17	Bingol	358	0.90	13485	1.35	51	1.00	0.82	82	Ra/Vi	Rm	Ds
18	Bitlis	333	0.98	13859	1.31	61	0.86	0.82	55	Wi/Cr	PR	Ds
20	Burdur	236	0.68	652	1.93	210	0.00	0.41	39	Cr/Fo	Rm	Cs
21	Bursa	2019	0.22	7844	0.81	186	0.53	0.94	18	Fo	Rm/PR	Cs
22	Canakkale	1039	0.35	12516	1.05	118	0.88	0.24	45	Fo	PR/Rm	Cs
23	Cankiri	907	0.90	15236	1.31	167	0.57	0.65	36	Cr/Ra	PR	Ds
24	Corum	3417	1.05	141946	1.30	135	0.88	0.82	62	Cr	PR	Ds
25	Denizli	2206	0.18	8218	1.31	242	0.41	0.53	18	Cr/Fo	Rm/PR	Cs
26	Diyarbakir	14319	0.78	1689028	0.80	126	0.94	0.82	76	Cr	PR/RI	Cs
28	Edirne	2321	0.46	128413	0.74	89	1.00	0.12	21	Cr	PR/RI	Cs
29	Elazig	800	0.74	11846	0.95	149	0.77	0.88	34	Vi/Ra	Rm	Ds
30	Erzincan	220	0.72	9316	0.92	60	1.00	0.76	41	Vi/Ra	Rm	Ds
31	Erzurum	290	0.75	3064	1.03	85	1.00	0.76	34	Ra/Vi	PR	Df/Ds
32	Eskisehir	1701	0.90	26150	2.03	182	0.50	0.24	35	Cr	PR	Ds/Cs
33	Gaziantep	3035	0.55	68203	0.67	114	0.94	1.00	54	Cr/Vi	RI/Rm	Cs
36	Hakkari	933	1.03	53729	1.22	92	0.67	0.82	80	Vi	Rm	Ds
37	Hatay	3781	0.41	95122	0.84	109	0.76	0.88	58	Fo/Cr	RI	Cs
38	Igdir	358	0.33	15405	1.11	189	0.40	0.29	48	Vi	RI	Df/B
39	Isparta	499	0.47	7871	2.07	131	0.62	0.88	37	Cr	Rm	Cs/Ds
40	Istanbul	478	0.62	1063	1.73	105	0.90	0.76	30	Fo	PR	Cs
41	Izmir	2879	0.22	40706	0.90	183	0.41	0.88	77	Fo/Cr	Rm/RI	Cs
42	K. Maras	4004	0.40	119380	0.78	125	0.59	0.76	47	Cr/Vi	Rm	Ds
43	Karabuk	430	0.77	782	3.40	162	0.63	0.59	21	Fo	Rm	Cf/Ds
44	Karaman	1197	0.70	26780	1.18	168	0.79	0.24	34	Cr/Vi	Rm	Ds/Cs
47	Kayseri	1749	0.81	41070	1.52	148	0.63	0.53	39	Cr	PR	Ds
48	Kilis	238	0.82	1953	1.50	88	0.83	0.94	39	Cr/Vi	PR/RR	Cs
49	Kinkkale	2649	1.04	180235	1.22	123	0.94	0.71	58	Cr	PR	Ds
50	Kirklarmli	714	0.48	4244	0.85	102	0.88	0.65	32	Cr/Fo	PR	Cs
51	Kirsehir	3358	1.11	234297	1.40	123	0.88	0.76	59	Cr	RI	Ds
52	Kocaeli	227	0.70	535	2.51	74	1.00	0.88	86	Fo	PR	Cs
53	Konya	13503	0.83	731153	1.24	194	0.76	0.53	49	Cr	PR	Ds
54	Kutahya	292	0.77	6059	1.46	118	0.75	0.65	35	Cr/Fo	PR/Rm	Cs/Ds
55	Malatya	649	0.43	4152	1.32	165	0.62	0.47	29	Vi	PR	Ds
56	Manisa	2334	0.39	81907	1.01	96	1.00	0.18	33	Cr/Fo	Rm	Cs
57	Mardin	16598	0.60	1381891	0.67	154	0.88	0.94	78	Cr	RI	Cs
58	Mersin	3439	0.31	53762	1.03	103	0.88	1.00	58	Fo	Rm	Cs
59	Mugla	681	0.47	15357	1.39	117	0.71	0.94	180	Fo	Rm	Cs
60	Mus	629	1.54	61588	2.39	71	0.89	0.63	58	Cr/Ra	PR	Ds
61	Nevsehir	1999	1.27	168902	1.42	79	0.93	0.71	67	Cr	PR	Ds
62	Nigde	416	0.60	2094	2.15	131	0.67	0.59	35	Cr/Vi	PR	Ds
64	Osmaniye	5501	0.21	342683	0.53	101	0.71	1.00	60	Fo/Cr	RI	Cs
66	Sakarya	706	0.51	6144	1.18	85	0.80	0.35	29	Fo	RI	Cf
67	Samsun	544	0.58	6999	1.45	105	0.82	0.18	16	Fo	PR	Cf
68	Sanliurfa	21139	0.62	1491819	0.59	176	0.88	0.94	69	Cr	RI	Cs
69	Siirt	1178	0.72	120922	0.94	60	1.00	0.82	60	Cr/Vi	Rm	Cs/Ds
71	Sirnak	2894	0.68	242368	0.72	92	0.88	1.00	78	Vi/Cr	Rm	Cs/Ds
72	Sivas	2435	0.80	95001	1.26	100	0.94	0.65	57	Vi/Cr	PR	Ds
73	Tekirdag	1705	0.62	11306	1.59	141	0.59	0.88	35	Cr	PR	Cs

74	Tokat	560	0.86	13444	1.14	55	1.00	0.82	43	Fo/Cr	RI/Rm	Ds
76	Tunceli	236	0.77	5892	0.91	58	0.80	0.71	61	Fo/Vi	Rm	Ds
77	Usak	1403	0.53	36250	1.38	132	0.71	0.88	26	Cr	PR	Cs
80	Yozgat	6257	1.18	493758	1.32	119	0.82	0.71	76	Cr	PR	Ds

Tab. C 1. List of the *sensu lato* and *sensu stricto* variables for each of the selected Turkish provinces.

*Vi*: Villages; *Wi*: Wildlands; *Cr*: Croplands; *Ra*: Rangelands; *Fo*: Forests.

*RI*: Residential Irrigated; *RR*: Residential Rainfed; *PR*: Populated Rainfed; *Rm*: Remote.

*B*: Arid; *Cf*: Temperate, w/out dry summer; *Cs*: Temperate, dry summer; *Df*: Cold, w/out dry summer; *Ds*: Cold, dry summer.

#### Appendix D: Correlation between the quantitative variables

	ICAF	CVAF	ICAB	CVAB	SL	MT	PSPM	IT
ICAF	1.00	-0.09	0.91	-0.37	0.23	0.08	0.26	0.20
CVAF	-0.09	1.00	0.03	0.40	-0.30	0.32	0.05	0.18
ICAB	0.91	0.03	1.00	-0.33	0.16	0.16	0.23	0.25
CVAB	-0.37	0.40	-0.33	1.00	0.04	-0.15	-0.08	0.03
SL	0.23	-0.30	0.16	0.04	1.00	-0.75	-0.18	-0.18
MT	0.08	0.32	0.16	-0.15	-0.75	1.00	0.15	0.16
PSPM	0.26	0.05	0.23	-0.08	-0.18	0.15	1.00	0.42
IT	0.20	0.18	0.25	0.03	-0.18	0.16	0.42	1.00

Tab. D 1. Correlations between the quantitative variables.